Available on CMS information server

CMS NOTE 2011/254

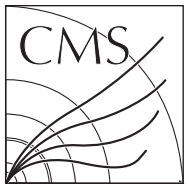

The Compact Muon Solenoid Experiment

CMS Note

Mailing address: CMS CERN, CH-1211 GENEVA 23, Switzerland

February 7, 2013

Searches for beyond-the-standard model physics in events with a Z boson, jets and missing transverse energy

D. Barge, C. Campagnari, D. Kovalskyi, V. Krutelyov

University of California, Santa Barbara, USA

W. Andrews, G. Cerati, D. Evans, F. Golf, I. MacNeill, S. Padhi, V. Welke, Y. Tu, F. Würthwein, A. Yagil, J. Yoo

University of California, San Diego, USA

L. Bauerdick, K. Burkett, I. Fisk, Y. Gao, O. Gutsche, B. Hooberman, S. Jindariani, J. Linacre, V. Martinez Outschoorn

Fermi National Accelerator Laboratory, Batavia, Illinois, USA

Abstract

This note describes a search for beyond-the-standard model (BSM) physics in events with a leptonically-decaying Z boson, jets, and missing transverse energy ($\mathrm{E_T^{miss}}$). This signature is predicted to occur in several BSM scenarios, for example supersymmetric (SUSY) models. Two search strategies are pursued. The first is an inclusive approach which selects events with at least two jets and large $\mathrm{E_T^{miss}}$, produced in association with the Z$\rightarrow \ell\ell$ candidate. The second is a targeted search in which additional requirements are imposed in order to achieve sensitivity to the production of the weakly-coupled SUSY charginos and neutralinos. The main backgrounds of SM $\mathrm{Z} + \mathrm{jets}$ and $t\bar{t}$ production are estimated with the data-driven $\mathrm{E_T^{miss}}$ templates technique and the opposite-flavor subtraction technique, respectively. Additional backgrounds are estimated from simulation, after validation in data control samples. In both the inclusive and targeted analyses, good agreement is observed between the data and predicted background over the full $\mathrm{E_T^{miss}}$ range.

Contents

1 Changes w.r.t. previous AN Version

- v9: Added description of signal efficiency uncertainties (Sec. 8). Added detailed summary of systematic uncertainties in the $\mathrm{E_T^{miss}}$ templates prediction (Sec. 6.1.1), including the MC closure study (App. A). Added plots requested by Petar in his review for the pre-approval. Cosmetic improvements to the targeted analysis "money plot" Fig. 11, including reduction of the (previously over-estimated) systematic uncertainty in the $\mathrm{E_T^{miss}} < 60$ GeV region.
- v8: Add studies of PU variable beta in App. B. Small (few %) change to $\mathrm{E_T^{miss}}$ templates prediction from fixing issue related to prescalees of the single photon triggers.
- v7: Add rejection of PU jets using the beta variable. Update the trigger efficiencies using measurements of the full 2012 sample. Update the data sample to the full 19.5 fb^{-1}. Correct the cross sections for the ZZZ and ZZJetsTo2L2Q MC samples.
- v6: Updated experimental results based on full 2012 sample, corresponding to 19.3 fb^{-1}.
- v5: **This is the version corresponding to the HCP results**. Added interpretation for the GMSB model. Added data vs. MC kinematic distributions for the sample with 3 leptons and at least 2 jets, where we observe an excess of data with respect to the MC prediction.
- v4: Un-blinded the results of the inclusive and targeted analysis, and added an interpretation in the WZ + $\mathrm{E_T^{miss}}$ model. Moved the material for the edge analysis to a separate AN (2012/359).
- v3: Added results for the low-$\mathrm{E_T^{miss}}$ and high-$\mathrm{E_T^{miss}}$ signal regions used for the edge analysis, for the first 5.1 fb^{-1} 2012A+B data.
- v2: Updated to 9.2 fb^{-1} of 53X data and MC (v1 used 5.1 fb^{-1} 52X data and MC).

2 Introduction

This note presents two searches for beyond-the-standard model (BSM) physics in events containing a leptonically-decaying Z boson, jets, and missing transverse energy. This is an update of previous searches performed with 2011 data [1, 2]. The search is based on a data sample of pp collisions collected at $\sqrt{s} = 8$ TeV in 2012, corresponding to an integrated luminosity of 19.5 fb^{-1}.

The production of Z bosons is expected in many BSM scenarios, for example supersymmetric (SUSY) models. In SUSY models with neutralino lightest SUSY particle (LSP), Z bosons may be produced in the decays $\chi_2^0 \to Z\chi_1^0$, where χ_2^0 is the second lightest neutralino and χ_1^0 is the lightest neutralino. In models with gravitino LSP such as gauge-mediated SUSY breaking (GMSB) models, Z bosons may be produced via $\chi_1^0 \to Z\tilde{G}$, where $\tilde{G}$ is the gravitino. Such decays may occur either in the cascade decays of the strongly-produced squarks and gluinos, or via direct production of the electroweak charginos and neutralino. Examples of such processes (see Fig. 1) are:

- strong production: $pp \to \tilde{g}\tilde{g} \to (q\bar{q}\chi_2^0)(q\bar{q}\chi_2^0) \to (q\bar{q}Z\chi_1^0)(q\bar{q}Z\chi_1^0) \to$ ZZ + 4 jets + $\mathrm{E_T^{miss}}$
- electroweak production: $pp \to \chi_1^\pm\chi_2^0 \to (W\chi_1^0)(Z\chi_1^0) \to$ WZ + $\mathrm{E_T^{miss}}$

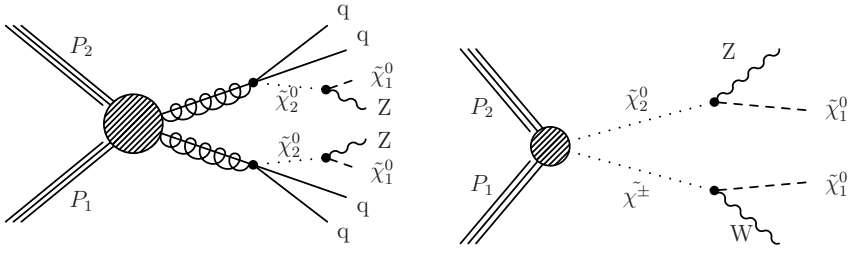

Figure 1: Examples of BSM physics signatures targeted in this search. In the left diagram, Z bosons are produced in the cascade decays of the strongly-interacting gluinos. In the right diagram, a Z boson is produced via direct production of the weakly-coupled charginos and neutralinos.

We thus pursue two strategies. The first is an inclusive strategy which selects events with a Z$\rightarrow \ell\ell$ candidate, at least two jets, and large $\mathrm{E_T^{miss}}$. This strategy is useful for targeting, e.g., the production of Z bosons in the cascade decays of strongly-interacting particles as depicted in Fig. 1 (left). In the second strategy, we impose additional requirements which strongly suppress the backgrounds while retaining high efficiency for events with Z bosons produced via direct production of the weakly-coupled charginos and neutralinos. These two strategies are referred to as the "inclusive search" and the "targeted search," respectively.

After selecting events with jets and a Z$\rightarrow \ell^+\ell^-$ ($\ell = e, \mu$) candidate, the dominant background consists of SM Z production accompanied by jets from initial-state radiation (Z + jets). The $\mathrm{E_T^{miss}}$ in $\mathrm{Z + jets}$ events arises primarily when jet energies are mismeasured. The $\mathrm{Z + jets}$ cross section is several orders of magnitude larger than our signal, and the artificial $\mathrm{E_T^{miss}}$ is not necessarily well reproduced in simulation. Therefore, the critical prerequisite to a discovery of BSM physics in the $Z + \mathrm{jets} + \mathrm{E_T^{miss}}$ final state is to establish that a potential excess is not due to SM $\mathrm{Z + jets}$ production accompanied by artificial $\mathrm{E_T^{miss}}$ from jet mismeasurements. In this note, the $\mathrm{Z + jets}$ background is estimated with the $\mathrm{E_T^{miss}}$templates technique, in which the artificial $\mathrm{E_T^{miss}}$in $\mathrm{Z + jets}$ events is modeled using a $\gamma + \mathrm{jets}$ control sample. The second background category consists of processes which produce leptons with uncorrelated flavor. These "flavor-symmetric" (FS) backgrounds, which are dominated by $t\bar{t}$ but also contain WW, DY$\rightarrow \tau\tau$ and single top processes, are estimated using a data control sample of eμ events. Additional backgrounds from WZ and ZZ production are estimated from MC, after validation of the MC modeling of these processes using 3-lepton and 4-lepton data control samples.

3 Datasets and Triggers

In this section we list the datasets, triggers, and MC samples used in the analysis. For selecting signal events, we use dilepton triggers in the DoubleElectron, DoubleMu, and MuEG datasets. An event in the ee final state is required to pass the dielectron trigger, a $\mu\mu$ event is required to pass the dimuon trigger, while an eμ event is required to pass at least one of the two $e-\mu$ cross triggers. The efficiencies of the ee and eμ triggers with respect to the offline selection with two $p_T > 20$ GeV have been measured as 0.95 ± 0.03, 0.93 ± 0.03, respectively. The $\mu\mu$ trigger efficiency is 0.90 ± 0.03 for events with two muons satisfying $|\eta| < 1$, and 0.81 ± 0.03 otherwise (the average trigger efficiency is 0.86 ± 0.03). A sample of $\gamma + \text{jets}$ events, used as a control sample to estimate the $\text{Z} + \text{jets}$ background, is selected using a set of single photon triggers. The golden prompt reco json and rereco jsons are merged, yielding an integrated luminosity of 19.5 fb^{-1}.

- Datasets
  - `DoubleElectron`
  - `DoubleMu`
  - `MuEG`
- Datasets
  - `Run2012A-13Jul2012-v1`
  - `Run2012A-recover-06Aug2012-v1`
  - `Run2012B-13Jul2012-v1`
  - `Run2012C-24Aug2012-v1`
  - `Run2012C-PromptReco-v2`
  - `MuEG_Run2012D-PromptReco-v1`
- Triggers
  - `HLT_Mu17_Mu8_v*`
  - `HLT_Mu17_Ele8_CaloIdT_CaloIsoVL_TrkIdVL_TrkIsoVL_v*`
  - `HLT_Mu8_Ele17_CaloIdT_CaloIsoVL_TrkIdVL_TrkIsoVL*`
  - `HLT_Ele17_CaloIdT_CaloIsoVL_TrkIdVL_TrkIsoVL_Ele8_CaloIdT_CaloIsoVL_TrkIdVL_TrkIsoVL_v*`
  - `HLT_Photon22_R9Id90_HE10_Iso40_EBOnly_v*`
  - `HLT_Photon36_R9Id90_HE10_Iso40_EBOnly_v*`
  - `HLT_Photon50_R9Id90_HE10_Iso40_EBOnly_v*`
  - `HLT_Photon75_R9Id90_HE10_Iso40_EBOnly_v*`
  - `HLT_Photon90_R9Id90_HE10_Iso40_EBOnly_v*`

Table 1: List of MC samples.

Process	Dataset Name	Cross Section [pb]
$\text{Z} + \text{jets}$	/DYJetsToLL_M-50_TuneZ2Star_8TeV-madgraph-tarball/Summer12_DR53X-PU_S10_START53_V7A-v1/AODSIM	3532.8
$t\bar{t}$	/TTJets_MassiveBinDECAY_TuneZ2star_8TeV-madgraph-tauola/Summer12_DR53X-PU_S10_START53_V7A-v1/AODSIM	225.2
ZZ	/ZZJetsTo4L_TuneZ2star_8TeV-madgraph-tauola/Summer12_DR53X-PU_S10_START53_V7A-v1/AODSIM	0.1769
	/ZZJetsTo2L2Q_TuneZ2star_8TeV-madgraph-tauola/Summer12_DR53X-PU_S10_START53_V7A-v1/AODSIM	2.4487
	/ZZJetsTo2L2Nu_TuneZ2star_8TeV-madgraph-tauola/Summer12_DR53X-PU_S10_START53_V7A-v3/AODSIM	0.3648
WZ	/WZJetsTo3LNu_TuneZ2_8TeV-madgraph-tauola/Summer12_DR53X-PU_S10_START53_V7A-v1/AODSIM	1.0575
	/WZJetsTo2L2Q_TuneZ2star_8TeV-madgraph-tauola/Summer12_DR53X-PU_S10_START53_V7A-v1/AODSIM	2.206
WW	/WWJetsTo2L2Nu_TuneZ2star_8TeV-madgraph-tauola/Summer12_DR53X-PU_S10_START53_V7A-v1/AODSIM	5.8123
single top	/T_tW-channel-DR_TuneZ2star_8TeV-powheg-tauola/Summer12_DR53X-PU_S10_START53_V7A-v1/AODSIM	11.177
	/Tbar_tW-channel-DR_TuneZ2star_8TeV-powheg-tauola/Summer12_DR53X-PU_S10_START53_V7A-v1/AODSIM	11.177
ttV	/TTZJets_8TeV-madgraph_v2/Summer12_DR53X-PU_S10_START53_V7A-v1/AODSIM	0.208
	/TTWJets_8TeV-madgraph/Summer12_DR53X-PU_S10_START53_V7A-v1/AODSIM	0.232
VVV	/ZZZNoGstarJets_8TeV-madgraph/Summer12_DR53X-PU_S10_START53_V7A-v1/AODSIM	0.0055
	/WWWJets_8TeV-madgraph/Summer12_DR53X-PU_S10_START53_V7A-v1/AODSIM	0.08217
	/WWZNoGstarJets_8TeV-madgraph/Summer12_DR53X-PU_S10_START53_V7A-v1/AODSIM	0.0633
	/WZZNoGstarJets_8TeV-madgraph/Summer12_DR53X-PU_S10_START53_V7A-v1/AODSIM	0.01922

4 Selection

In this section, we list the event selection, electron and muon objects selections, jets, $\mathrm{E_T^{miss}}$, and b-tagging selections used in this analysis. These selections are based on those recommended by the relevant POG's.

4.1 Event Selection

We require the presence of at least one primary vertex satisfying the standard quality criteria; namely, vertex is not fake, $\mathrm{ndf} \geq 4$, $\rho < 2$ cm, and $|z| < 24$ cm.

4.2 Lepton Selection

Because $\mathrm{Z} \to \ell\ell$ ($\ell = e, \mu$) is a final state with very little background, we restrict ourselves to events in which the Z boson decays to electrons or muons only. Therefore opposite sign leptons passing the identification and isolation requirements described below are required in each event.

- $p_T > 20$ GeV and $|\eta| < 2.4$;
- Opposite-sign same-flavor (SF) ee and $\mu\mu$ lepton pairs (opposite-flavor (OF) eμ lepton pairs are retained in a control sample used to estimate the FS contribution);
- For SF events, the dilepton invariant mass is required to be consistent with the Z mass; namely $81 < m_{\ell\ell} < 101$ GeV.

4.2.1 Electron Selection

The electron selection is the loose working point recommended by the E/gamma POG, as documented at [3]. Electrons with $p_T > 20$ GeV and $|\eta| < 2.4$ are considered. We use PF-based isolation with a cone size of $\Delta R < 0.3$, using the effective area rho corrections documented at [4], and we require a relative isolation < 0.15. Electrons in the transition region defined by $1.4442 < |\eta_{SC}| < 1.566$ are rejected. Electrons with a selected muon with $p_T > 10$ GeV within $\Delta R < 0.1$ are rejected. The electron selection requirements are listed in Table 2 for completeness.

Table 2: Summary of the electron selection requirements.

Quantity	Barrel	Endcap
$\delta\eta$	< 0.007	< 0.009
$\delta\phi$	< 0.15	< 0.10
$\sigma_{i\eta i\eta}$	< 0.01	< 0.03
H/E	< 0.12	< 0.10
d_0 (w.r.t. 1st good PV)	< 0.02 cm	< 0.02 cm
d_z (w.r.t. 1st good PV)	< 0.2 cm	< 0.2 cm
$\lvert 1/E - 1/P \rvert$	< 0.05 GeV^{-1}	< 0.05 GeV^{-1}
PF isolation / p_T	< 0.15	< 0.15
conversion rejection: fit probability	$< 10^{-6}$	$< 10^{-6}$
conversion rejection: missing hits	≤ 1	≤ 1

4.2.2 Muon Selection

We use the tight muon selection recommended by the muon POG, as documented at [5]. Muons with $p_T > 20$ GeV and $|\eta| < 2.4$ are considered. We use PF-based isolation with a cone size of $\Delta R < 0.3$, using the $\Delta\beta$ PU correction scheme, and we require a relative isolation of < 0.15. The muon selection requirements are listed in Table 3 for completeness.

4.3 Photons

As will be explained later, it is not essential that we select real photons. What is needed are jets that are predominantly electromagnetic, well measured in the ECAL, and hence less likely to contribute to fake MET. We select photons with:

Table 3: Summary of the muons selection requirements.

Quantity	Requirement
muon type	global muon and PF muon
χ^2/ndf	< 10
muon chamber hits	≥ 1
matched stations	≥ 2
d_0 (w.r.t. 1st good PV)	< 0.02 cm
d_z (w.r.t. 1st good PV)	< 0.5 cm
pixel hits	≥ 1
tracker layers	≥ 5

- $p_T > 22$ GeV
- $|\eta| < 2$
- $H/E < 0.1$
- No matching pixel track (pixel veto)
- There must be a pfjet of $p_T > 10$ GeV matched to the photon within $dR < 0.3$. The matched jet is required to have a neutral electromagnetic energy fraction of at least 70%.
- We require that the pfjet p_T matched to the photon satisfy (pfjet p_T - photon p_T) > -5 GeV. This removes a few rare cases in which "overcleaning" of a pfjet generates fake MET.
- We also match photons to calojets and require (calojet p_T - photon p_T) > -5 GeV (the same requirement used for pfjets). This is to remove other rare cases in which fake energy is added to the photon object but not the calojet.
- We reject photons which have an electron of at least $p_T > 10$ GeV within $dR < 0.2$ in order to reject conversions from electrons from W decays which are accompanied by real MET.
- We reject photons which are aligned with the MET to within 0.14 radians in phi.

4.4 MET

We use pfmet, henceforth referred to simply as $\mathrm{E_T^{miss}}$.

4.5 Jets

- PF jets with L1FastL2L3 corrections (MC), L1FastL2L3residual corrections (data).
- $|\eta| < 2.5$
- Passes loose PFJet ID
- $p_T > 30$ GeV for determining the jet multiplicity, $p_T > 15$ GeV for calculation of H_T
- For the creation of photon templates, the jet matched to the photon passing the photon selection described above is vetoed
- For the dilepton sample, jets are vetoed if they are within $\Delta R < 0.4$ from any lepton $p_T > 20$ GeV passing analysis selection
- To reject PU jets, we require the jets to satisfy $\beta > 0.2$, defined for each jet using the d_Z of the tracks in the jet with respect to the primary vertex (see App. B for further details). To calculate β we take the sum of the p_T^2 of the tracks associated to PFCandidates in the jet that are consistent with originating from the primary vertex ($d_Z < 0.5$ cm), and divide by the sum p_T^2 of all the tracks:

$$\beta = \frac{\Sigma_i^{\mathrm{d_z}<0.5\ \mathrm{cm}}(p_T^i)^2}{\Sigma_i^{\mathrm{all}}(p_T^i)^2} \tag{1}$$

- A jet is considered as "b-tagged" if it passes the above criteria and the CSV medium working point.

5 Data vs. MC Comparison in Preselection Region

In this section we compare the data and MC samples passing the selection described in Sec. 4 In the following, the MC is reweighted to match the data distribution of number of reconstructed primary vertices. The trigger efficiencies of Sec. 3 are applied. In all plots, the last bin contains the overflow. Note that we show here data vs. MC comparisons as a sanity check only, since the dominant backgrounds estimated from data.

We begin by counting the inclusive Z yields. Here we require the presence of two selected leptons without any additional requirements on jets or $\mathrm{E_T^{miss}}$. In Fig. 2 the distribution of dilepton invariant mass in the ee and $\mu\mu$ channels is displayed. In Table 4 the yields for selected dilepton events in the Z mass window are indicated. Good data vs. MC agreement is observed, within the systematic uncertainties of integrated luminosity (4.5%), trigger efficiency (3%), $\mathrm{Z}+\mathrm{jets}$ and $t\bar{t}$ cross sections.

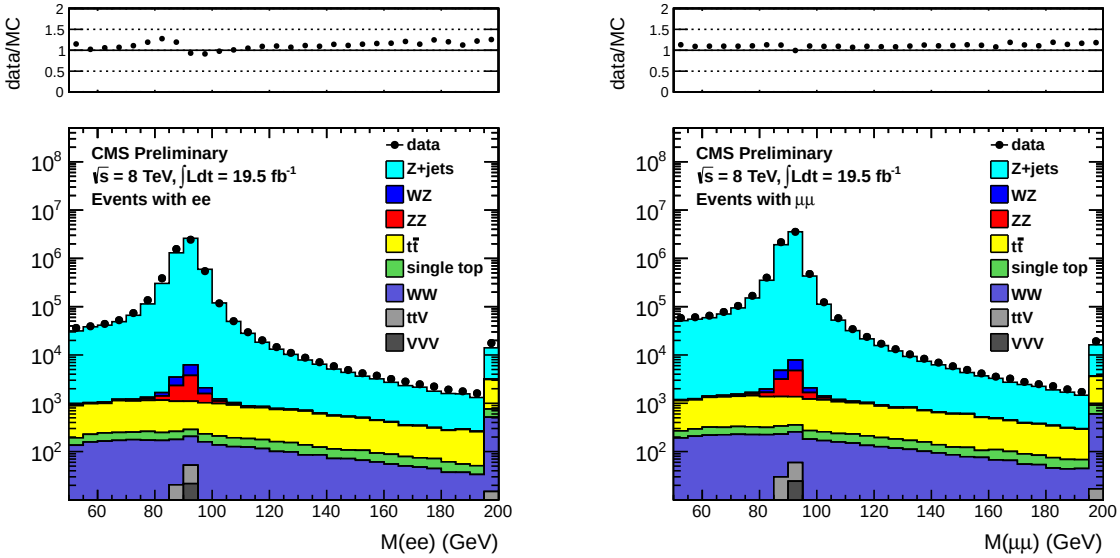

Figure 2: Dilepton mass distribution for events with two selected leptons in the ee (left) and $\mu\mu$ (right) final states.

Table 4: Data and Monte Carlo yields for events with two selected leptons in the Z mass window.

Sample	ee	$\mu\mu$	eμ	total
$\mathrm{Z}+\mathrm{jets}$	4776593 ± 3391	6227613 ± 3627	2328 ± 73.9	11006533 ± 4966
$t\bar{t}$	3321.1 ± 45.8	4014.4 ± 47.6	7621.3 ± 68.7	14956.8 ± 95.3
WW	614.8 ± 6.0	773.7 ± 6.3	1433.1 ± 9.0	2821.7 ± 12.6
WZ	4342.7 ± 7.3	5411.7 ± 7.7	115.3 ± 1.1	9869.7 ± 10.6
ZZ	4712.8 ± 9.9	5906.1 ± 10.5	21.0 ± 0.3	10639.8 ± 14.4
single top	315.3 ± 11.9	388.4 ± 12.4	709.5 ± 17.6	1413.2 ± 24.6
$t\bar{t}\mathrm{V}$	57.4 ± 1.1	68.1 ± 1.1	21.8 ± 0.7	147.3 ± 1.7
VVV	30.1 ± 0.3	36.4 ± 0.4	6.9 ± 0.2	73.5 ± 0.5
total SM MC	4789987.0 ± 3391.1	6244211.0 ± 3627.1	12256.7 ± 102.8	11046454.7 ± 4966.5
data	4906970	6552612	13141	11472723

We next define the preselection region for the inclusive search using the following requirements:

- Number of jets ≥ 2;
- Same flavor dileptons (opposite flavor yields will be shown since they are used in data for the FS background estimation);
- Dilepton invariant mass $81 < m_{\ell\ell} < 101$ GeV.

The dilepton mass distributions in the preselection region of the inclusive search (without the dilepton mass requirement applied) for the ee and $\mu\mu$ final states are shown in Figure 3. In Table 5 the data and MC yields in the inclusive preselection region are indicated. Good data vs. MC agreement is observed.

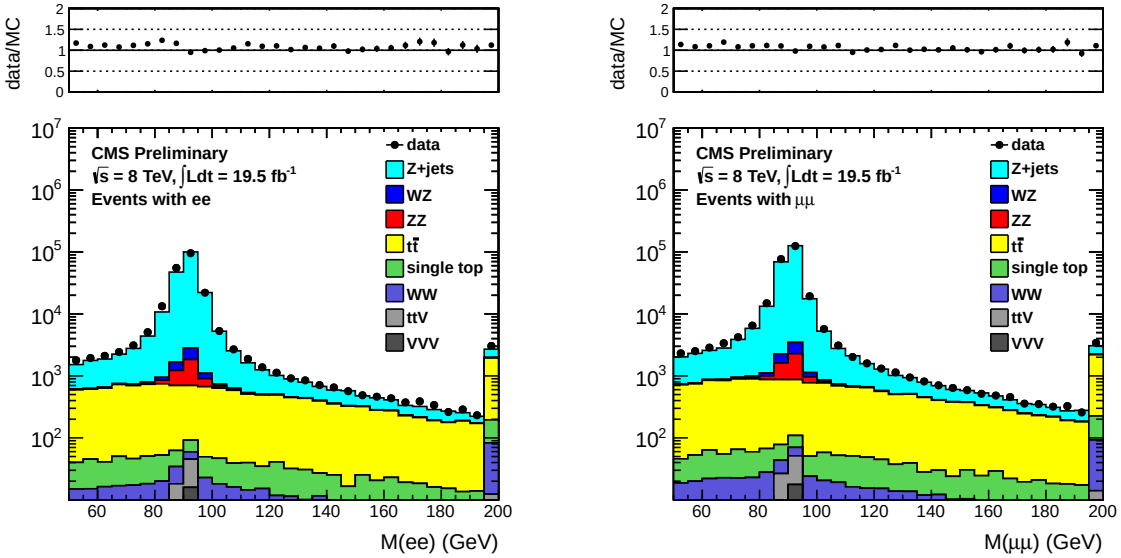

Figure 3: Dilepton mass distribution for events in the preselection region of the inclusive search in the ee (left) and $\mu\mu$ (right) final states.

Table 5: Data and MC yields in the preselection region of the inclusive search.

Sample	ee	$\mu\mu$	eμ	total
Z + jets	174022.4 ± 645.0	218277.0 ± 678.9	86.9 ± 14.4	392386.4 ± 936.5
$t\bar{t}$	2536.3 ± 40.1	3058.7 ± 41.6	5824.7 ± 60.1	11419.7 ± 83.3
WW	59.5 ± 1.9	73.2 ± 1.9	134.2 ± 2.8	266.9 ± 3.9
WZ	1709.7 ± 4.7	2098.1 ± 4.9	20.0 ± 0.4	3827.8 ± 6.8
ZZ	2002.4 ± 6.9	2477.2 ± 7.2	4.2 ± 0.2	4483.8 ± 9.9
single top	121.2 ± 7.4	137.7 ± 7.4	263.7 ± 10.7	522.6 ± 15.0
$t\bar{t}$V	54.9 ± 1.0	65.6 ± 1.1	20.0 ± 0.6	140.5 ± 1.6
VVV	21.7 ± 0.3	26.2 ± 0.3	3.4 ± 0.1	51.3 ± 0.4
total SM MC	180528.1 ± 646.4	226213.8 ± 680.2	6357.1 ± 62.7	413098.9 ± 940.4
data	185555	234132	6231	425918

We next define the preselection region for the targeted search by adding the following requirements:

- Veto events containing a b-tagged jet;
- Dijet invariant mass $70 < m_{jj} < 110$ GeV;
- Veto events containing a third selected lepton (electron or muon) with $p_T > 10$ GeV;

The rejection of events with a b-tagged jet strongly suppresses the $t\bar{t}$ background, which is the dominant background in the inclusive search after requiring large $\mathrm{E_T^{miss}}$. The requirement that the jet pair is consistent with originating from W/Z decay is motivated by the fact that we are searching for signatures producing V(jj)Z($\ell\ell$)+$\mathrm{E_T^{miss}}$; this requirement suppresses the $\mathrm{Z} + \mathrm{jets}$ and $t\bar{t}$ backgrounds. The veto of events containting a third electron or muon suppresses the WZ background, and also serves to make this analyis exclusive with respect to searches in the trilepton final state.

The dilepton mass distributions in the preselection region of the targeted search (without the dilepton mass requirement applied) for the ee and $\mu\mu$ final states are shown in Figure 4. In Table 6 the data and MC yields in the preselection region are indicated. Good data vs. MC agreement is observed. We also show the distribution of dijet mass in the targeted preselection (with the requirement on this quantity removed) in Fig. 5, which demonstrates that the MC does a reasonable job of modeling this quantity. The dijet mass selection efficiency for data and MC is quantified in Table 7.

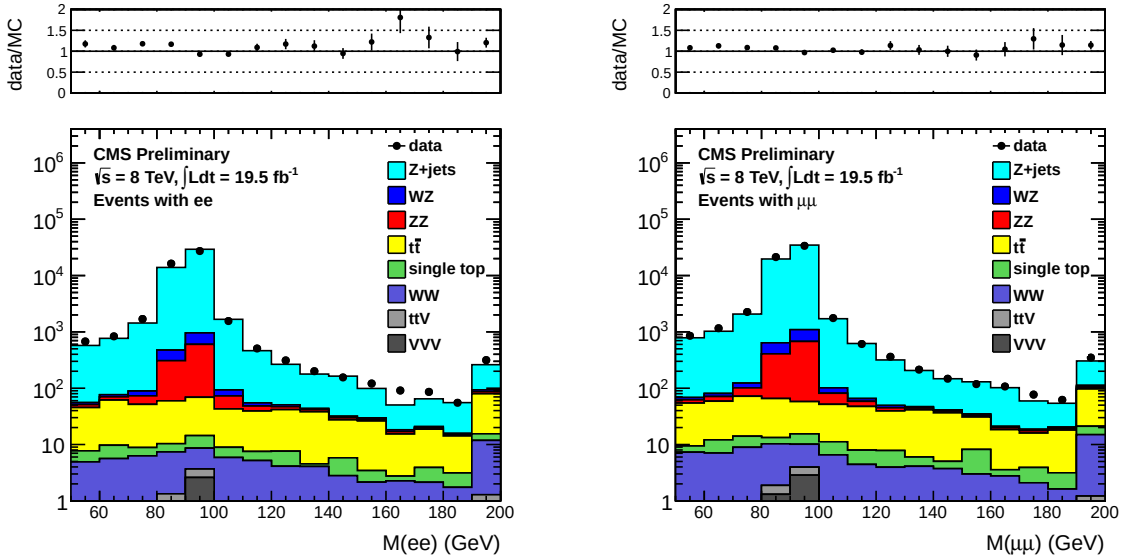

Figure 4: Dilepton mass distribution for events in the preselection region of the targeted search in the ee (left) and $\mu\mu$ (right) final states.

Table 6: Data and MC yields in the preselection region of the targeted search.

Sample	ee	$\mu\mu$	eμ	total
$\mathrm{Z} + \mathrm{jets}$	41811.7 ± 316.2	52620.2 ± 333.3	19.4 ± 6.9	94451.2 ± 459.4
$t\bar{t}$	99.9 ± 8.0	95.8 ± 7.3	215.1 ± 11.5	410.8 ± 15.8
WW	11.0 ± 0.8	14.1 ± 0.8	25.8 ± 1.2	50.9 ± 1.7
WZ	525.4 ± 2.6	648.5 ± 2.7	3.1 ± 0.2	1177.0 ± 3.8
ZZ	779.2 ± 4.3	957.9 ± 4.5	0.8 ± 0.1	1737.9 ± 6.3
single top	9.1 ± 2.1	8.7 ± 1.8	14.0 ± 2.4	31.9 ± 3.7
$t\bar{t}\mathrm{V}$	1.6 ± 0.2	1.7 ± 0.2	0.8 ± 0.1	4.1 ± 0.3
VVV	3.4 ± 0.1	4.2 ± 0.1	0.9 ± 0.1	8.5 ± 0.2
total SM MC	43241.2 ± 316.3	54351.0 ± 333.4	280.0 ± 13.7	97872.2 ± 459.8
data	43444	54851	275	98570

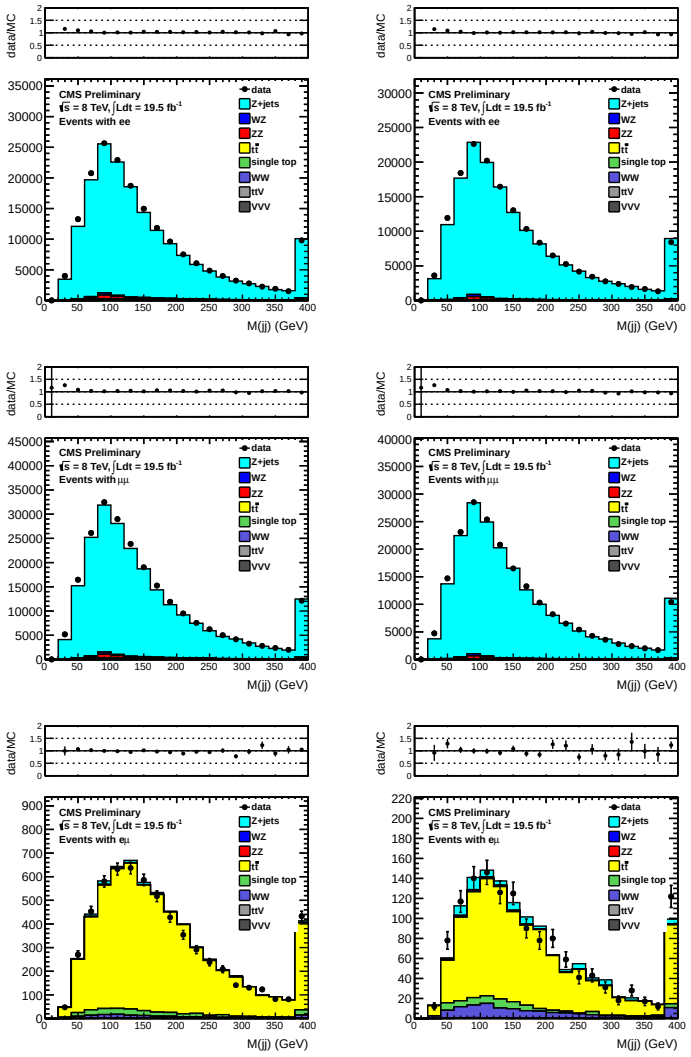

Figure 5: Distributions of dijet mass for the inclusive preselection (left) and targeted preselection (right), in the ee (top), $\mu\mu$ (middle) and eμ (bottom) final state.

Table 7: Data and MC selection efficiencies for the dijet mass (m_{jj}) requirement, with respect to the inclusive preselection.

Sample	ee	$\mu\mu$	eμ
MC (inclusive)	180528.1 $\pm$ 646.4	226213.8 $\pm$ 680.2	6357.1 $\pm$ 62.7
MC (inclusive + m_{jj} requirement)	48466.6 $\pm$ 333.3	61162.1 $\pm$ 352.1	1124.8 $\pm$ 26.5
MC efficiency	26.8%	27.0%	17.7%
Data (inclusive)	185555	234132	6231
Data (inclusive + m_{jj} requirement)	49256	62414	1131
Data efficiency	26.5%	26.7%	18.2%

6 Background Estimation Techniques

In this section we describe the techniques used to estimate the SM backgrounds in our signal regions defined by requirements of large $\mathrm{E_T^{miss}}$. The SM backgrounds fall into three categories:

- $\mathrm{Z} + \mathrm{jets}$: this is the dominant background after the preselection. The $\mathrm{E_T^{miss}}$ in $\mathrm{Z} + \mathrm{jets}$ events is estimated with the "$\mathrm{E_T^{miss}}$ templates" technique described in Sec. 6.1;
- Flavor-symmetric (FS) backgrounds: this category includes processes which produces 2 leptons of uncorrelated flavor. It is dominated by $t\bar{t}$ but also contains Z$\rightarrow \tau\tau$, WW, and single top processes. This is the dominant contribution in the signal regions, and it is estimated using a data control sample of eμ events as described in Sec. 6.2;
- WZ and ZZ backgrounds: this background is estimated from MC, after validating the MC modeling of these processes using data control samples with jets and exactly 3 leptons (WZ control sample) and exactly 4 leptons (ZZ control sample) as described in Sec. 6.3;

6.1 Estimating the $\mathrm{Z} + \mathrm{jets}$ Background with $\mathrm{E_T^{miss}}$ Templates

The premise of this data driven technique is that $\mathrm{E_T^{miss}}$ in $\mathrm{Z} + \mathrm{jets}$ events is produced by the hadronic recoil system and *not* by the leptons making up the Z. Therefore, the basic idea of the $\mathrm{E_T^{miss}}$ template method is to measure the $\mathrm{E_T^{miss}}$ distribution in a control sample which has no true MET and the same general attributes regarding fake MET as in $\mathrm{Z} + \mathrm{jets}$ events. We thus use a sample of $\gamma + \mathrm{jets}$ events, since both $\mathrm{Z} + \mathrm{jets}$ and $\gamma + \mathrm{jets}$ events consist of a well-measured object recoiling against hadronic jets.

For selecting photon-like objects, the very loose photon selection described in Sec. 4.3 is used. It is not essential for the photon sample to have high purity. For our purposes, selecting jets with predominantly electromagnetic energy deposition in a good fiducial volume suffices to ensure that they are well measured and do not contribute to fake $\mathrm{E_T^{miss}}$. The $\gamma + \mathrm{jets}$ events are selected with a suite of single photon triggers with p_T thresholds varying from 22–90 GeV. The events are weighted by the trigger prescale such that $\gamma + \mathrm{jets}$ events evenly sample the conditions over the full period of data taking. There remains a small difference in the PU conditions in the $\gamma + \mathrm{jets}$ vs. $\mathrm{Z} + \mathrm{jets}$ samples due to the different dependencies of the γ vs. Z isolation efficiencies on PU. To account for this, we reweight the $\gamma + \mathrm{jets}$ samples to match the distribution of reconstructed primary vertices in the $\mathrm{Z} + \mathrm{jets}$ sample.

To account for kinematic differences between the hadronic systems in the control vs. signal samples, we measure the $\mathrm{E_T^{miss}}$ distributions in the $\gamma + \mathrm{jets}$ sample in bins of the number of jets and the scalar sum of jet transverse energies (H_T). These $\mathrm{E_T^{miss}}$ templates are extracted separately from the 5 single photon triggers with thresholds 22, 36, 50, 75, and 90 GeV, so that the templates are effectively binned in photon p_T . All $\mathrm{E_T^{miss}}$distributions are normalized to unit area to form "MET templates". The prediction of the MET in each Z event is the template which corresponds to the N_{jets}, H_T, and Z p_T in the $\mathrm{Z} + \mathrm{jets}$ event. The prediction for the Z sample is simply the sum of all such templates. All templates are displayed in App. D.

After preselection, there is a small contribution from backgrounds other than $\mathrm{Z} + \mathrm{jets}$. To correct for this, the $\mathrm{E_T^{miss}}$ templates prediction is scaled such that the total background prediction matches the observed data yield in the $\mathrm{E_T^{miss}}$ 0–60 GeV region. Because the non-$\mathrm{Z} + \mathrm{jets}$ impurity in the low $\mathrm{E_T^{miss}}$ region after preselection is very small, this results in scaling factors of 0.985 (0.995) for the inclusive (targeted) search.

6.1.1 Systematic Uncertainty in the $\mathrm{E_T^{miss}}$ Templates Prediction

In this section we consider the systematic uncertainty in the $\mathrm{E_T^{miss}}$ templates prediction, which comes from 3 sources: an MC closure study (see App. A), variation of the photon selection criteria, and the nvtx reweighting procedure. We seperate the systematic uncertainty into 2 regions: $\mathrm{E_T^{miss}} < 60$ GeV (where the $\mathrm{E_T^{miss}}$ templates prediction is normalized such that the total background prediction matches the data yield), and $\mathrm{E_T^{miss}} > 60$ GeV. These uncertainties apply to the targeted analysis used for the ewkino analysis.

From the results obtained in the closure test, we assign an uncertainty of 1% to the $\mathrm{E_T^{miss}} < 60$ GeV region, 20% to the $\mathrm{E_T^{miss}}$ 60–80 GeV region, and 30% to $\mathrm{E_T^{miss}} > 80$ GeV region, where the 30% is uncertainty is based on the largest statistically significant deviation in the large $\mathrm{E_T^{miss}}$ regions.

Next, we asses the uncertainties associated with the photon selections. We vary the H/E selection by tightening it to $H/E < 0.05$, and $H/E < 0.01$ and recalculating the predictions from the $\mathrm{E_T^{miss}}$ templates. From these results,

we assign a 2% systematic uncertainty to the region with $\mathrm{E_T^{miss}} < 60$ GeV, and a 10% systematic uncertainty to the regions with $\mathrm{E_T^{miss}} > 60$ GeV for the H/E selection.

Although the pileup conditions in the signal $\mathrm{Z}+\mathrm{jets}$ and control $\gamma+\mathrm{jets}$ events are the same, the photon isolation criteria introduce a bias which causes the nvtx distributed in the selected $\mathrm{Z}+\mathrm{jets}$ and $\gamma+\mathrm{jets}$ events to differ. As described above, we reweight the $\gamma+\mathrm{jets}$ sample to reproduce the nvtx distribution in the $\mathrm{Z}+\mathrm{jets}$ sample. To assess the corresponding uncertainty, we calculate the $\mathrm{E_T^{miss}}$ templates prediction without reweighting, and take half the difference from the nominal prediction as the systematic uncertainty. This results in a systematic uncertainty of 3% for the $\mathrm{E_T^{miss}} < 60$ GeV region, and 10% for the $\mathrm{E_T^{miss}} > 60$ GeV region.

A summary comparing the nominal $\mathrm{E_T^{miss}}$ templates prediction to the ones obtained by varying the H/E criteria and removing the nvtx reweighting is presented in Table 8. A summary of the assessed systematic uncertainties on the $\mathrm{E_T^{miss}}$ templates prediction is summarized in Table 9. The total systematic uncertainty on the $\mathrm{E_T^{miss}}$ templates prediction is 4% for $\mathrm{E_T^{miss}} < 60$ GeV, 22% for $\mathrm{E_T^{miss}}$ 60–80 GeV, and 33% for $\mathrm{E_T^{miss}} > 80$ GeV.

Table 8: Results from varying the H/T photon selection, and removing the vertex reweighting done when making the $\mathrm{E_T^{miss}}$ templates. The errors shown here are statistical only.

	$0 < \mathrm{E_T^{miss}} < 30$	$30 < \mathrm{E_T^{miss}} < 60$	$60 < \mathrm{E_T^{miss}} < 80$	$80 < \mathrm{E_T^{miss}} < 100$
Nominal Yields	75834 $\pm$ 232.2	21232 $\pm$ 117.7	690 $\pm$ 19.0	64.5 $\pm$ 5.8
$H/T < 0.05$	76246.9 $\pm$ 232.6	20834.8 $\pm$ 123.8	647.5 $\pm$ 21.6	60.8 $\pm$ 5.6
% change	0.6 $\pm$ 0.4	1.8 $\pm$ 0.8	6.1 $\pm$ 4.46	5.8 $\pm$ 12.5
$H/T < 0.01$	76355.1 $\pm$ 248.3	20730.0 $\pm$ 132.3	641.0 $\pm$ 23.0	63.5 $\pm$ 6.4
% change	0.7 $\pm$ 0.5	2.3 $\pm$ 0.9	7.1 $\pm$ 4.6	1.4 $\pm$ 13.7
No reweighting	77308.5 $\pm$ 228.7	19869.0 $\pm$ 113.5	559.6 $\pm$ 16.9	53.0 $\pm$ 4.4
% change	2.0 $\pm$ 0.4	6.4 $\pm$ 0.77	18.9 $\pm$ 3.7	17.8 $\pm$ 10.5
	$100 < \mathrm{E_T^{miss}} < 120$	$120 < \mathrm{E_T^{miss}} < 150$	$150 < \mathrm{E_T^{miss}} < 200$	$200 < \mathrm{E_T^{miss}}$
Nominal Yields	7.8 $\pm$ 1.8	3.7 $\pm$ 1.1	2.0 $\pm$ 0.7	0.4 $\pm$ 0.3
$H/T < 0.05$	7.5 $\pm$ 1.7	3.6 $\pm$ 1.1	2.1 $\pm$ 0.7	0.4 $\pm$ 0.3
% change	3.6 $\pm$ 30.7	2.7 $\pm$ 42.0	3.6 $\pm$ 53.2	2.1 $\pm$ 99.1
$H/T < 0.01$	7.8 $\pm$ 1.9	3.3 $\pm$ 1.2	2.3 $\pm$ 0.8	0.5 $\pm$ 0.3
% change	0.2 $\pm$ 33.2	9.5 $\pm$ 43.4	17.2 $\pm$ 60.1	10.0 $\pm$ 111.3
No reweighting	7.3 $\pm$ 1.6	3.7 $\pm$ 1.1	2.1 $\pm$ 0.7	0.4 $\pm$ 0.3
% change	6.5 $\pm$ 29.2	1.4 $\pm$ 43.3	3.4 $\pm$ 52.9	9.1 $\pm$ 91.8

Table 9: Summary table of the systematic uncertainty in the $\mathrm{E_T^{miss}}$ templates prediction. All values are relative uncertainties, in %.

Source	$0 < \mathrm{E_T^{miss}} < 60$ GeV	$60 < \mathrm{E_T^{miss}} < 80$ GeV	$\mathrm{E_T^{miss}} > 60$
MC closure	1	10	30
Photon selection	2	20	10
nvtx reweighting	3	10	10
Total	4	22	33

6.2 Estimating the Flavor-Symmetric Background with eμ Events

In this subsection we describe the background estimate for the FS background. Since this background produces equal rates of same-flavor (SF) ee and $\mu\mu$ lepton pairs as opposite-flavor (OF) eμ lepton pairs, the OF yield can be used to estimate the SF yield, after correcting for the different electron vs. muon offline selection efficiencies and the different efficiencies for the ee, $\mu\mu$, and eμ triggers.

An important quantity needed to translate from the OF yield to a prediction for the background in the SF final state is the ratio $R_{\mu e} = \epsilon_\mu/\epsilon_e$, where ϵ_μ (ϵ_e) indicates the offline muon (electron) selection efficiency. This quantity can be extracted from data using the observed Z$\rightarrow \mu\mu$ and Z$\rightarrow$ee yields in the preselection region, after correcting for the different trigger efficiencies.

Hence we define:

- $N_{ee}^{\mathrm{trig}} = \epsilon_{ee}^{\mathrm{trig}} N_{ee}^{\mathrm{offline}}$,
- $N_{\mu\mu}^{\mathrm{trig}} = \epsilon_{\mu\mu}^{\mathrm{trig}} N_{\mu\mu}^{\mathrm{offline}}$,
- $N_{e\mu}^{\mathrm{trig}} = \epsilon_{e\mu}^{\mathrm{trig}} N_{e\mu}^{\mathrm{offline}}$.

Here $N_{\ell\ell}^{\mathrm{trig}}$ denotes the number of selected Z events in the $\ell\ell$ channel passing the offline and trigger selection (in other words, the number of recorded and selected events), $\epsilon_{\ell\ell}^{\mathrm{trig}}$ is the trigger efficiency, and $N_{\ell\ell}^{\mathrm{offline}}$ is the number

of events that would have passed the offline selection if the trigger had an efficiency of 100%. Thus we calculate the quantity:

$$R_{\mu e} = \sqrt{\frac{N_{\mu\mu}^{\rm offline}}{N_{ee}^{\rm offline}}} = \sqrt{\frac{N_{\mu\mu}^{\rm trig}/\epsilon_{\mu\mu}^{\rm trig}}{N_{ee}^{\rm trig}/\epsilon_{ee}^{\rm trig}}} = \sqrt{\frac{234132/0.86}{185555/0.95}} = 1.18 \pm 0.07. \quad (2)$$

Here we have used the Z$\rightarrow \mu\mu$ and Z$\rightarrow$ee yields from Table 5 and the trigger efficiencies quoted in Sec. 3. The indicated uncertainty is due to the 3% uncertainties in the trigger efficiencies. The predicted yields in the ee and $\mu\mu$ final states are calculated from the observed eμ yield as

- $N_{ee}^{\rm predicted} = \frac{N_{e\mu}^{\rm trig}}{\epsilon_{e\mu}^{\rm trig}} \frac{\epsilon_{ee}^{\rm trig}}{2R_{\mu e}} = \frac{N_{e\mu}^{\rm trig}}{0.93} \frac{0.95}{2\times 1.18} = (0.43 \pm 0.05) \times N_{e\mu}^{\rm trig}$,
- $N_{\mu\mu}^{\rm predicted} = \frac{N_{e\mu}^{\rm trig}}{\epsilon_{e\mu}^{\rm trig}} \frac{\epsilon_{\mu\mu}^{\rm trig} R_{\mu e}}{2} = \frac{N_{e\mu}^{\rm trig}}{0.95} \frac{0.86\times 1.18}{2} = (0.53 \pm 0.07) \times N_{e\mu}^{\rm trig}$,

and the predicted yield in the combined ee and $\mu\mu$ channel is simply the sum of these two predictions:

- $N_{ee+\mu\mu}^{\rm predicted} = (0.97 \pm 0.06) \times N_{e\mu}^{\rm trig}$.

Note that the relative uncertainty in the combined ee and $\mu\mu$ prediction is smaller than those for the individual ee and $\mu\mu$ predictions because the uncertainty in $R_{\mu e}$ cancels when summing the ee and $\mu\mu$ predictions.

To improve the statistical precision of the FS background estimate, we remove the requirement that the eμ lepton pair falls in the Z mass window. Instead we scale the eμ yield by K, the efficiency for eμ events to satisfy the Z mass requirement, extracted from simulation. In Fig. 6 we display the value of K in data and simulation, for a variety of $\rm E_T^{miss}$ requirements, for the inclusive analysis. Based on this we chose $K = 0.14 \pm 0.02$ for the lower $\rm E_T^{miss}$ regions, $K = 0.14 \pm 0.04$ for the $\rm E_T^{miss} > 200$ GeV region, and $K = 0.14 \pm 0.08$ for $\rm E_T^{miss} > 300$ GeV, where the larger uncertainties reflect the reduced statistical precision at large $\rm E_T^{miss}$. The corresponding plot for the targeted analysis, including the b-veto, is displayed in Fig. 7. Based on this we chose $K = 0.13 \pm 0.02$ for all $\rm E_T^{miss}$ regions up to $\rm E_T^{miss} > 100$ GeV. For the $\rm E_T^{miss} > 150$ GeV region we choose $K = 0.13 \pm 0.03$ and for the $\rm E_T^{miss} > 200$ GeV region we choose $K = 0.13 \pm 0.05$, due to the reduced statistical precision.

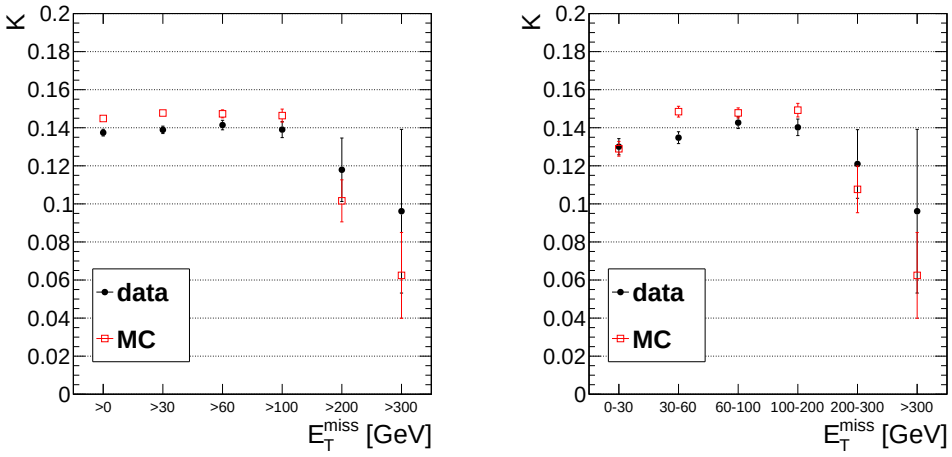

Figure 6: The efficiency for eμ events to satisfy the dilepton mass requirement, K, in data and simulation for inclusive $\rm E_T^{miss}$ intervals (left) and exclusive $\rm E_T^{miss}$ intervals (right) for the inclusive analysis. Based on this we chose $K = 0.14 \pm 0.02$ for the lower $\rm E_T^{miss}$ regions, $K = 0.14 \pm 0.04$ for the $\rm E_T^{miss} > 200$ GeV region, and $K = 0.14 \pm 0.08$ for $\rm E_T^{miss} > 300$ GeV.

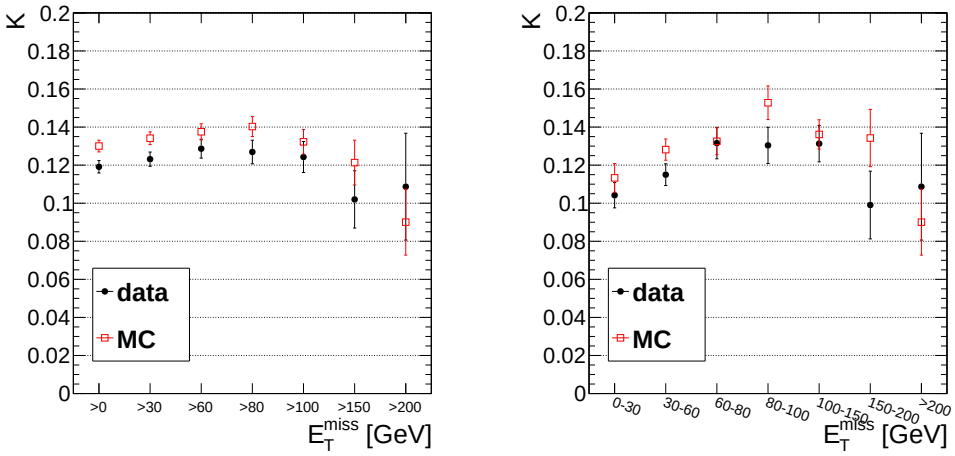

Figure 7: The efficiency for eμ events to satisfy the dilepton mass requirement, K, in data and simulation for inclusive $\mathrm{E_T^{miss}}$ intervals (left) and exclusive $\mathrm{E_T^{miss}}$ intervals (right) for the targeted analysis, including the b-veto. Based on this we chose $K = 0.13 \pm 0.02$ for the $\mathrm{E_T^{miss}}$ regions up to $\mathrm{E_T^{miss}} > 100$ GeV. For $\mathrm{E_T^{miss}} > 150$ we choose $K = 0.13 \pm 0.03$, for $\mathrm{E_T^{miss}} > 200$ GeV we choose $K = 0.13 \pm 0.05$.

6.3 Estimating the WZ and ZZ Background with MC

Backgrounds from W($\ell\nu$)Z($\ell\ell$) where the W lepton is not identified or is outside acceptance, and Z($\nu\nu$)Z($\ell\ell$), are estimated from simulation. The MC modeling of these processes is validated by comparing the MC predictions with data in control samples with exactly 3 leptons (WZ control sample) and exactly 4 leptons (ZZ control sample). The critical samples are the WZJetsTo3LNu and ZZJetsTo4L, listed in Table 1 (the WZJetsTo2L2Q, ZZJetsTo2L2Q, and ZZJetsTo2L2Nu samples are also used in this analysis but their contribution to the 3-lepton and 4-lepton control samples is negligible).

6.3.1 WZ Validation Studies

A pure WZ sample can be selected in data with the requirements:

- Exactly 3 $p_T > 20$ GeV leptons passing analysis identication and isolation requirements,
- 2 of the 3 leptons must fall in the Z window 81-101 GeV,
- $\mathrm{E_T^{miss}} > 50$ GeV (to suppress DY),
- veto events with b-tagged jets.

The data and MC yields passing the above selection are in Table 10. The inclusive yields (without any jet requirements) in the same-flavor final states (660 observed vs. 596 ± 5.2 MC expected) agree within 11%, which is consistent within the $\approx$15% uncertainty in the theory prediction for the WZ cross section. A data vs. MC comparison of kinematic distributions (jet multiplicity, $\mathrm{E_T^{miss}}$, Z p_T) is given in Fig. 8. High $\mathrm{E_T^{miss}}$ values in WZ and ZZ events arise from highly boosted W or Z bosons that decay leptonically, and we therefore check that the MC does a reasonable job of reproducing the p_T distributions of the leptonically decaying Z . While the inclusive WZ yields are in reasonable agreement, we observe an excess in data in events with at least 2 jets, corresponding to the jet multiplicity requirement in our preselection. We observe 124 same-flavor events in data while the MC predicts 88 ± 1.5 (stat), representing an excess of 41%, as indicated in Table 11, and we therefore assess an uncertainty of 50% on the WZ background.

Table 10: Data and Monte Carlo yields passing the WZ preselection.

Sample	ee	$\mu\mu$	eμ	total
WZ	244.0 ± 1.6	301.8 ± 1.6	17.0 ± 0.4	562.8 ± 2.3
ZZ	10.2 ± 0.1	12.8 ± 0.1	0.8 ± 0.0	23.8 ± 0.1
Z + jets	3.3 ± 2.4	5.8 ± 3.4	0.0 ± 0.0	9.0 ± 4.2
$t\bar{t}$	0.6 ± 0.6	4.5 ± 1.6	2.1 ± 1.1	7.3 ± 2.0
single top	0.0 ± 0.0	0.5 ± 0.5	0.0 ± 0.0	0.5 ± 0.5
WW	0.0 ± 0.0	0.1 ± 0.1	0.2 ± 0.1	0.3 ± 0.1
ttV	2.3 ± 0.2	2.6 ± 0.2	0.6 ± 0.1	5.5 ± 0.3
VVV	3.0 ± 0.1	3.7 ± 0.1	0.6 ± 0.1	7.4 ± 0.2
total SM MC	263.4 ± 3.0	331.8 ± 4.2	21.4 ± 1.2	616.6 ± 5.2
data	288	372	36	696

Table 11: Data and Monte Carlo yields passing the WZ preselection and $N_{\rm jets} \geq 2$.

Sample	ee	$\mu\mu$	eμ	total
WZ	33.0 ± 0.6	41.1 ± 0.6	2.3 ± 0.2	76.3 ± 0.9
ZZ	1.7 ± 0.0	2.1 ± 0.0	0.1 ± 0.0	3.9 ± 0.1
$\mathrm{Z} + \mathrm{jets}$	0.0 ± 0.0	0.0 ± 0.0	0.0 ± 0.0	0.0 ± 0.0
$t\bar{t}$	0.6 ± 0.6	1.3 ± 0.9	1.2 ± 0.9	3.1 ± 1.4
single top	0.0 ± 0.0	0.5 ± 0.5	0.0 ± 0.0	0.5 ± 0.5
WW	0.0 ± 0.0	0.0 ± 0.0	0.0 ± 0.0	0.0 ± 0.0
$t\bar{t}\mathrm{V}$	1.8 ± 0.2	2.1 ± 0.2	0.4 ± 0.1	4.3 ± 0.3
VVV	1.5 ± 0.1	2.0 ± 0.1	0.1 ± 0.0	3.7 ± 0.1
total SM MC	38.7 ± 0.9	49.1 ± 1.2	4.1 ± 0.9	91.8 ± 1.7
data	61	63	11	135

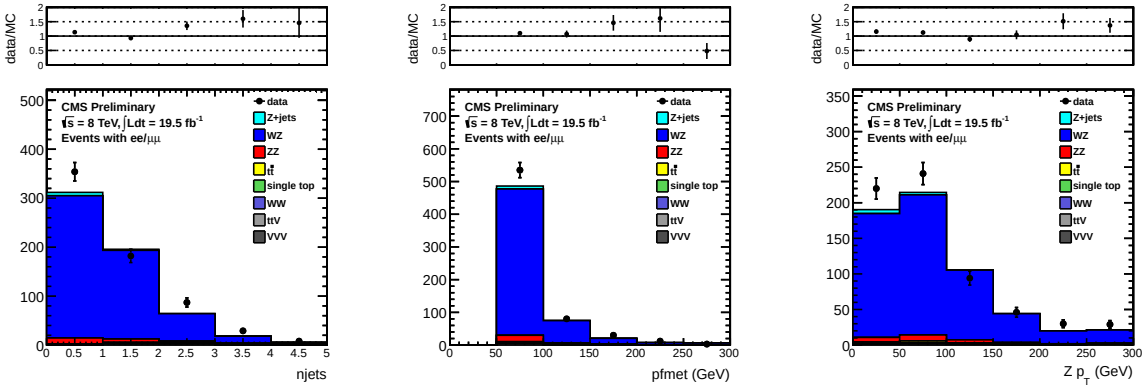

Figure 8: Data vs. MC comparisons for the WZ selection discussed in the text for 19.5 fb^{-1}. The number of jets, missing transverse energy, and Z boson transverse momentum are displayed.

6.3.2 ZZ Validation Studies

A pure ZZ sample can be selected in data with the requirements:

- Exactly 4 $p_T > 20$ GeV leptons passing analysis identication and isolation requirements,
- 2 of the 4 leptons must fall in the Z window 81-101 GeV.

The data and MC yields passing the above selection are in Table 12. In this ZZ-dominated sample we observe good agreement between the data yield and the MC prediction. After requiring 2 jets (corresponding to the requirement in the analysis selection), we observe 11 events in data and the MC predicts 11 ± 0.2 events. Due to the limited statistical precision we assign an uncertainty of 50% on the ZZ yield.

Table 12: Data and Monte Carlo yields for the ZZ preselection.

Sample	ee	$\mu\mu$	eμ	total
ZZ	53.0 ± 0.2	70.7 ± 0.2	3.5 ± 0.0	127.2 ± 0.3
$t\bar{t}$V	1.3 ± 0.2	1.4 ± 0.2	0.3 ± 0.1	3.0 ± 0.2
VVV	0.7 ± 0.1	0.9 ± 0.1	0.0 ± 0.0	1.7 ± 0.1
Z + jets	0.0 ± 0.0	0.0 ± 0.0	0.0 ± 0.0	0.0 ± 0.0
WZ	0.1 ± 0.0	0.1 ± 0.0	0.0 ± 0.0	0.3 ± 0.1
$t\bar{t}$	0.0 ± 0.0	0.0 ± 0.0	0.0 ± 0.0	0.0 ± 0.0
single top	0.0 ± 0.0	0.0 ± 0.0	0.0 ± 0.0	0.0 ± 0.0
WW	0.0 ± 0.0	0.0 ± 0.0	0.0 ± 0.0	0.0 ± 0.0
total SM MC	55.1 ± 0.3	73.1 ± 0.3	3.9 ± 0.1	132.1 ± 0.4
data	57	82	5	144

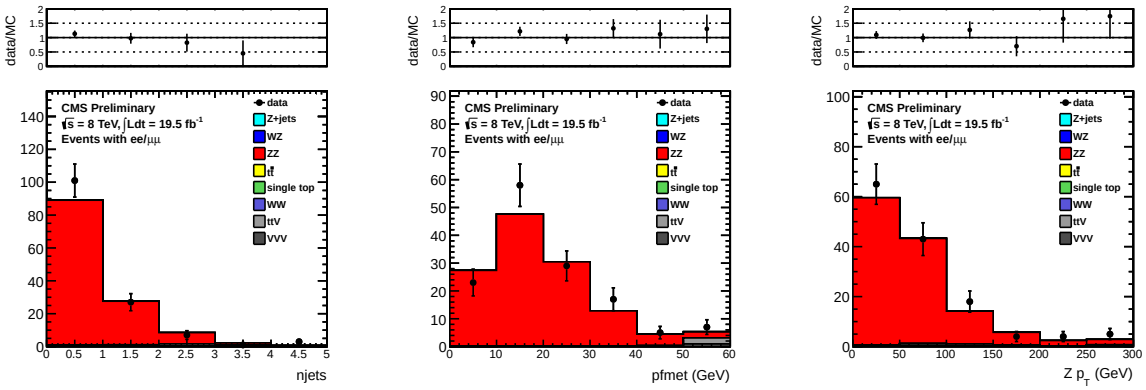

Figure 9: Data vs. MC comparisons for the ZZ selection discussed in the text for 19.5 fb^{-1}. The number of jets, missing transverse energy, and Z boson transverse momentum are displayed.

7 Results

In this section we provide the results of the inclusive and targeted searches. The observed and predicted $\mathrm{E_T^{miss}}$ distributions for the inclusive analysis are indicated in Fig. 10. A summary of the results in the signal regions is provided in Table 13. Good agreement is observed between the data and the predicted background over the full $\mathrm{E_T^{miss}}$ range. The separate results for the ee and $\mu\mu$ channels are presented in App. C.

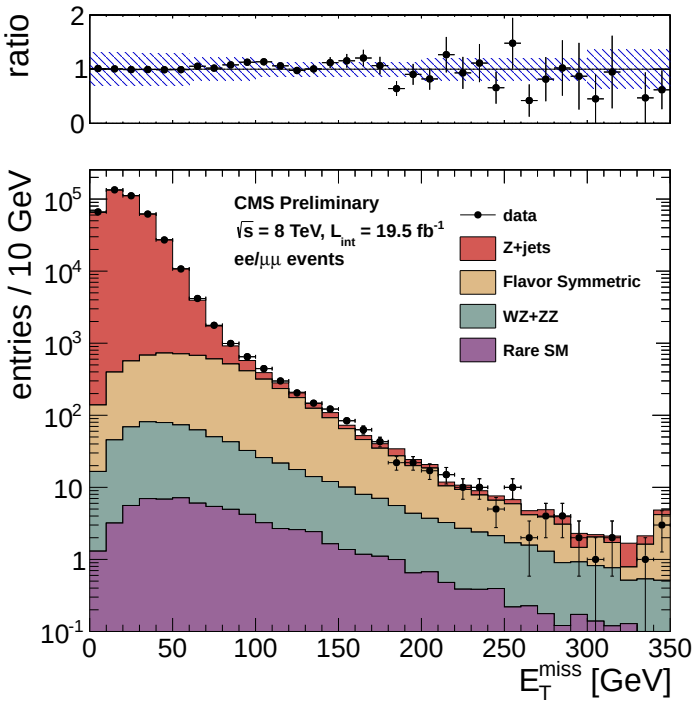

Figure 10: Results of the inclusive analysis. The observed $\mathrm{E_T^{miss}}$ distribution (black points) is compared with the sum of the predicted $\mathrm{E_T^{miss}}$ distributions from $\mathrm{Z}+\mathrm{jets}$, flavor-symmetric backgrounds, and WZ+ZZ backgrounds. The ratio of observed to predicted yields in each bin is indicated. The error bars indicate the statistical uncertainty in the data and the shaded band indicates the total background uncertainty.

Table 13: Summary of results in the inclusive analysis. The total background is the sum of the $\mathrm{Z}+\mathrm{jets}$ background predicted from the $\mathrm{E_T^{miss}}$ templates method ($\mathrm{Z}+\mathrm{jets}$ bkg), the flavor-symmetric background predicted from eμ events (FS bkg), and the WZ and ZZ backgrounds predicted from MC (WZ bkg and ZZ bkg). All uncertainties include both the statistical and systematic components. The Gaussian significance of the deviation between the data and total background is indicated for signal regions with at least 20 observed events.

	$\mathrm{E_T^{miss}}$ 0–30 GeV	$\mathrm{E_T^{miss}}$ 30–60 GeV	$\mathrm{E_T^{miss}}$ 60–100 GeV	$\mathrm{E_T^{miss}}$ 100–200 GeV	$\mathrm{E_T^{miss}}$ 200–300 GeV	$\mathrm{E_T^{miss}} > 300$ GeV
$\mathrm{Z}+\mathrm{jets}$ bkg	309185 ± 92757	98161 ± 29449	4971 ± 1492	222 ± 67	11.3 ± 3.5	2.6 ± 1.0
FS bkg	972 ± 151	1889 ± 293	2022 ± 314	1011 ± 157	50.7 ± 15.0	7.2 ± 4.3
WZ bkg	108.9 ± 54.5	186.4 ± 93.2	137.7 ± 68.9	78.7 ± 39.3	11.1 ± 5.6	3.1 ± 3.1
ZZ bkg	12.1 ± 6.1	26.6 ± 13.3	29.8 ± 14.9	29.8 ± 14.9	6.2 ± 3.1	2.0 ± 2.0
rare SM bkg	10.1 ± 5.1	21.0 ± 10.5	20.6 ± 10.3	17.9 ± 9.0	3.2 ± 1.6	1.1 ± 1.1
total bkg	310289 ± 92757	100284 ± 29451	7180 ± 1526	1360 ± 176	82.5 ± 16.8	16.0 ± 5.8
data	311030	99543	7578	1450	79	7

The observed and predicted $\mathrm{E_T^{miss}}$ distributions for the targeted analysis are indicated in Fig. 11. A summary of the results in the signal regions is provided in Table 14. Good agreement is observed between the data and the predicted background over the full $\mathrm{E_T^{miss}}$ range. The separate results for the ee and $\mu\mu$ channels are presented in App. C.

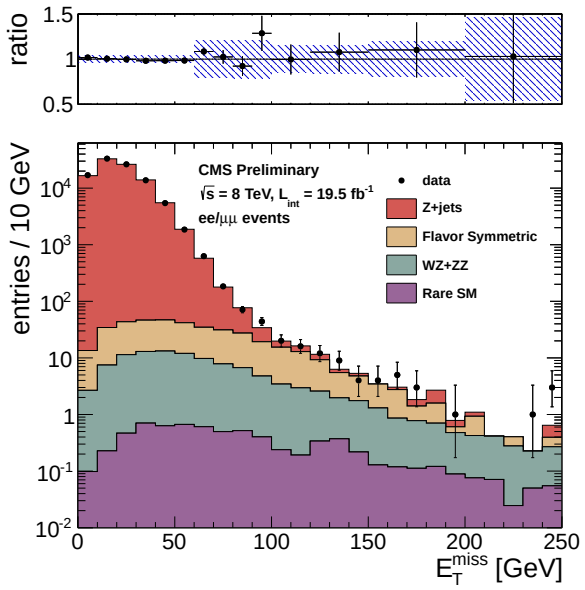

Figure 11: Results of the $\mathrm{Z}+\mathrm{dijet}$ analysis. The observed $\mathrm{E_T^{miss}}$ distribution (black points) is compared with the sum of the predicted $\mathrm{E_T^{miss}}$ distributions from $\mathrm{Z}+\mathrm{jets}$, flavor-symmetric (FS), sum of WZ and ZZ (WZ+ZZ), and rare SM backgrounds. The ratio of observed to predicted yields in each bin is indicated. The error bars indicate the statistical uncertainty in the data and the shaded band indicates the total background uncertainty.

Table 14: Summary of results in the targeted analysis. The total background is the sum of the $\mathrm{Z}+\mathrm{jets}$ background predicted from the $\mathrm{E_T^{miss}}$ templates method ($\mathrm{Z}+\mathrm{jets}$ bkg), the flavor-symmetric background predicted from eμ events (FS bkg), and the WZ and ZZ backgrounds predicted from MC (WZ bkg and ZZ bkg). All uncertainties include both the statistical and systematic components. The Gaussian significance of the deviation between the data and total background is indicated for signal regions with at least 20 observed events.

	$\mathrm{E_T^{miss}}$ 0–30 GeV	$\mathrm{E_T^{miss}}$ 30–60 GeV	$\mathrm{E_T^{miss}}$ 60–80 GeV	$\mathrm{E_T^{miss}}$ 80–100 GeV
$\mathrm{Z}+\mathrm{jets}$ bkg	75834 ± 3042	21232 ± 859	690 ± 154	64.5 ± 22.2
FS bkg	69.9 ± 11.9	96.7 ± 16.3	48.3 ± 8.3	35.2 ± 6.2
WZ bkg	17.7 ± 8.8	29.8 ± 14.9	13.0 ± 6.5	7.4 ± 3.7
ZZ bkg	3.1 ± 1.5	6.4 ± 3.2	3.5 ± 1.8	3.2 ± 1.6
Rare SM bkg	0.8 ± 0.4	2.0 ± 1.0	1.1 ± 0.6	0.9 ± 0.5
Total bkg	75926 ± 3042	21367 ± 859	756 ± 154	111 ± 23
Data	76302	20991	809	115
	$\mathrm{E_T^{miss}}$ 100–120 GeV	$\mathrm{E_T^{miss}}$ 120–150 GeV	$\mathrm{E_T^{miss}}$ 150–200 GeV	$\mathrm{E_T^{miss}} > 200$ GeV
$\mathrm{Z}+\mathrm{jets}$ bkg	7.8 ± 3.1	3.7 ± 1.6	2.0 ± 1.0	0.4 ± 0.3
FS bkg	21.9 ± 4.0	13.2 ± 2.5	5.7 ± 1.6	0.8 ± 0.4
WZ bkg	4.0 ± 2.0	3.3 ± 1.6	2.0 ± 1.0	0.9 ± 0.9
ZZ bkg	1.9 ± 1.0	2.1 ± 1.1	1.5 ± 0.8	1.4 ± 1.4
Rare SM bkg	0.4 ± 0.2	0.9 ± 0.5	0.6 ± 0.3	0.4 ± 0.4
Total bkg	36.1 ± 5.5	23.2 ± 3.6	11.8 ± 2.3	3.9 ± 1.8
Data	36	25	13	4

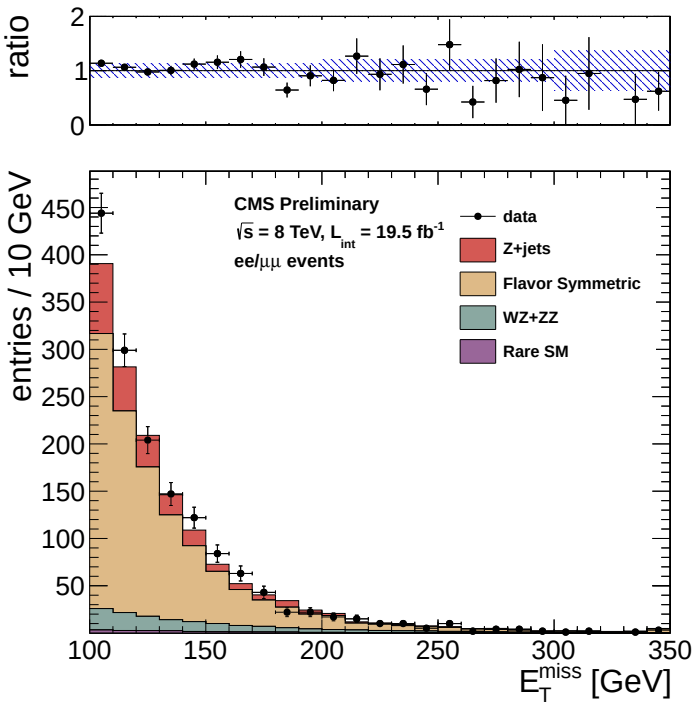

Figure 12: Results for the inclusive analysis, the same as Fig. 10 but zoomed in on the signal region $\mathrm{E_T^{miss}} > 100$ GeV and on linear scale.

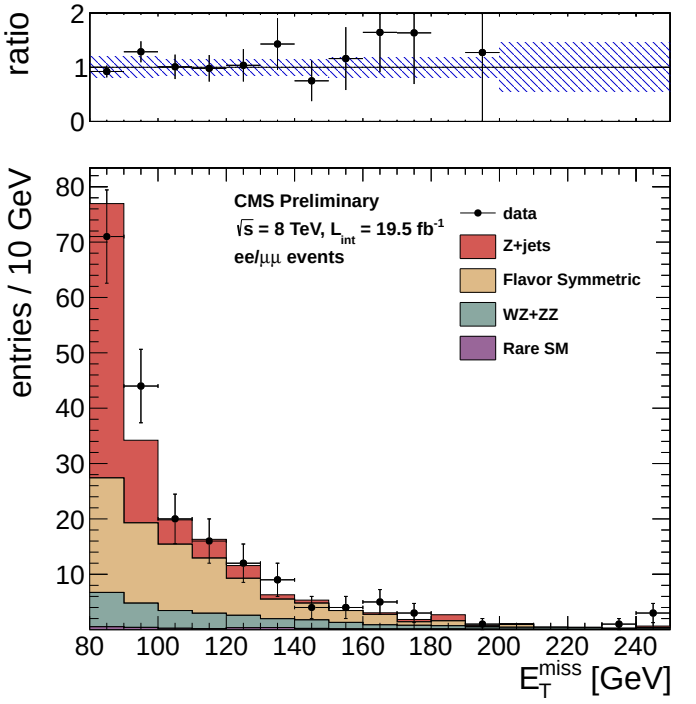

Figure 13: Results for the targeted analysis, the same as Fig. 11 but zoomed in on the signal region $\mathrm{E_T^{miss}} > 80$ GeV and on linear scale.

8 Systematic Uncertainties in Signal Acceptance

In this section we discuss systematic uncertainties in the signal acceptance. These efficiency uncertainties are relevant for the interpretations in the WZ + $\mathrm{E_T^{miss}}$ and the GMSB models, which are combined with the results of the trilepton and quadlepton analysis, respectively, in AN-2012/351.

Table 15: Summary of uncertainties in the signal efficiency.

Source	Value (%)	Method
Luminosity	4.4	official CMS value
Trigger efficiency	3	efficiency measurements documented in Sec. 4, Table 9 of AN-2012/248
Lepton ID/isolation	2 (per lepton)	Z tag-and-probe measurements in AN-2012/257
B-veto	6	dedicated measurement in AN-2012/248 Sec. 7.6
Z mass window requirement	3	see text and Table 16
Jet selection, dijet mass, $\mathrm{E_T^{miss}}$	assessed at each model point	official JetMet POG recipe

A summary of the efficiency uncertainties is presented in Table 15. The CMS uncertainty in the luminosity is 4.4%. The trigger efficiency is measured in AN-2102/248 with an uncertainty of 3%. The lepton identification and isolation requirements are measured in data and MC and found to be consistent within 2%, for the $p_T > 20$ GeV region relevant for this analysis, in AN-2012/257. The impact of the b-veto on the signal acceptance is quantified with a dedicated measurement performed in Sec. 7.6 of AN-2012/248. The uncertainty in the selection of dilepton events satisfying the Z mass window requirement 81–101 GeV is performed as follows. In both data and MC, the Z mass window in the inclusive preselection region (Z and at least 2 jets) is loosened to 60–120 GeV. The efficiency of the events in the loose window to satisfy the analysis dilepton mass selection of 81–101 GeV is compared in data and MC, and found to be consistent within 3% for both ee and $\mu\mu$ channels (see Table 16), and a corresponding uncertainty on the signal efficiency is assessed.

The above uncertainties are the same for all SUSY model points. However the impact of the jet energy scale uncertainty, which affects the selection efficiencies for all jets and $\mathrm{E_T^{miss}}$ objects, varies significantly across the model parameter space and is assessed separately at each point. The official JetMet POG recipe is used for this purpose. Each jet is assigned an uncertainty based on its p_T and η. The jet energy is varied by this uncertainty, which is propagated to the efficiencies for the jet selection, dijet mass selection and $\mathrm{E_T^{miss}}$ selection. In addition, for the $\mathrm{E_T^{miss}}$, a 10% uncertainty on the unclustered energy is included. The $\mathrm{E_T^{miss}}$ variation alters the shape of the signal $\mathrm{E_T^{miss}}$ distribution and causes a bin-to-bin migration of events, which is included in the limit setting procedure performed with LandS.

Table 16: Summary of the dilepton mass selection efficiency uncertainties. Loose and tight refer to dilepton mass windows of 60–120 GeV and 81-101 GeV, respectively.

	ee	$\mu\mu$
MC loose	190661.9	238969.2
MC tight	174162.5	218462.9
MC tight/loose	0.913 ± 0.005	0.914 ± 0.004
data loose	209540	263747
data tight	185555	234132
data tight/loose	0.886 ± 0.003	0.888 ± 0.003

9 Summary

This note presents a search for BSM physics in final states with leptonically-decaying Z bosons, jets, and $\mathrm{E_T^{miss}}$. Two strategies were pursued. The first is an inclusive approach which targets BSM scenarios with Z bosons produced in the decays of strongly-interacting particles. The second is a targeted approach which focuses on BSM scenarios where the Z bosons are produced in the decays of weakly-interacting particles. The main backgrounds are estimated with data-driven techniques. Good agreement is observed between the data and the predicted backgrounds over the full $\mathrm{E_T^{miss}}$ range, for both searches.

References

[1] CMS Collaboration, "Search for physics beyond the standard model in events with a Z boson, jets, and missing transverse energy in pp collisions at $\sqrt{s} = 7$ TeV,", arXiv:1204.3774v1 [hep-ex].

[2] SUS-12-006, paper draft

[3] https://twiki.cern.ch/twiki/bin/viewauth/CMS/EgammaCutBasedIdentification

[4] https://twiki.cern.ch/twiki/bin/viewauth/CMS/EgammaEARhoCorrection

[5] https://twiki.cern.ch/twiki/bin/view/CMSPublic/SWGuideMuonId

[6] M. Chen, AN 2012/237 "Interpretation of the Same-Sign di-leptons with bjets and MET search"

A Closure Test for Template Method

The E_T^{miss} template method is applied to MC to test its effectiveness under ideal conditions. We construct templates in MC using the procedure described in Sec. 6.1. The MC samples used for the construction of templates as well as the sample used for E_T^{miss} predictions is listed below. After these templates are constructed from the photon samples, they are then used to predict the E_T^{miss} distribution in Z + jets MC. The datasets used for the closure test are listed in table 17

Table 17: List of MC samples used for the closure test.

Process	Dataset Name	Cross Section [pb]
γ + Jets	/G_Pt-15to30_TuneZ2star_8TeV_pythia6/Summer12_DR53X-PU_S10_START53_V7A-v1/AODSIM	200061.7
	/G_Pt-30to50_TuneZ2star_8TeV_pythia6/Summer12_DR53X-PU_S10_START53_V7A-v1/AODSIM	19931.62
	/G_Pt-50to80_TuneZ2star_8TeV_pythia6/Summer12_DR53X-PU_S10_START53_V7A-v1/AODSIM	3322.309
	/G_Pt-80to120_TuneZ2star_8TeV_pythia6/Summer12_DR53X-PU_S10_START53_V7A-v1/AODSIM	558.2865
	/G_Pt-120to170_TuneZ2star_8TeV_pythia6/Summer12_DR53X-PU_S10_START53_V7A-v1/AODSIM	108.0068
	/G_Pt-170to300_TuneZ2star_8TeV_pythia6/Summer12_DR53X-PU_S10_START53_V7A-v1/AODSIM	30.12207
	/G_Pt-300to470_TuneZ2star_8TeV_pythia6/Summer12_DR53X-PU_S10_START53_V7A-v1/AODSIM	2.138632
	/G_Pt-470to800_TuneZ2star_8TeV_pythia6/Summer12_DR53X-PU_S10_START53_V7A-v1/AODSIM	0.2119244
	/G_Pt-800to1400_TuneZ2star_8TeV_pythia6/Summer12_DR53X-PU_S10_START53_V7A-v1/AODSIM	0.007077847
$Z + Jets$	/DYToEE_M-20_CT10_TuneZ2star_v2_8TeV-powheg-pythia6/Summer12_DR53X-PU_S10_START53_V7A-v1/AODSIM	1930.9940
	/DYToMuMu_M-20_CT10_TuneZ2star_v2_8TeV-powheg-pythia6/Summer12_DR53X-PU_S10_START53_V7A-v1/AODSIM	1930.9940

A.1 Selection

The same preselection requirements from the section 4 are used to study the closure of the template method, specifically:

- Require two leptons (OS, SF) which both pass the lepton selection with $p_T > 20$ GeV/c
- 81 GeV $< M_{\ell\ell} <$ 101 GeV
- Require at least two jets both with $p_T > 30$ GeV/c and $|\eta| < 2.5$

A.2 Results

The results of these tests are shown in Fig. 14, and Fig. 15. Additionally, the yields are listed in table 18, and table 19.

Table 18: Results of MC closure tests for the inclusive analysis selections listed in section 4. The first row shows the yields from the E_T^{miss} templates made from the photon sample. The second row shows the yield in DY MC. The third row shows the ratio of the DY Yield to the prediction from the templates. All uncertainties shown are statistical only.

	$0 < \mathrm{E_T^{miss}} < 30$	$30 < \mathrm{E_T^{miss}} < 60$	$60 < \mathrm{E_T^{miss}} < 100$	$100 < \mathrm{E_T^{miss}} < 200$	$200 < \mathrm{E_T^{miss}} < 300$	$\mathrm{E_T^{miss}} > 300$
Templates	221801.0 ± 943.7	55818.6 ± 493.2	2001.6 ± 66.4	78.1 ± 11.4	2.0 ± 0.18	0.7 ± 0.39
DY Yields	219941 ± 469.0	57483 ± 239.8	2212 ± 47.0	63 ± 7.9	3 ± 1.7	0 ± 1.0
MC/BG	99.2 ± 0.48 %	103.0 ± 0.98 %	110.5 ± 3.94 %	80.7 ± 19.24 %	146.6 ± 58.42 %	0.0 ± inf %

Table 19: Results of MC closure tests for the targeted analysis selections listed in section 4. The first row shows the yields from the E_T^{miss} templates made from the photon sample. The second row shows the yield in DY MC. The third row shows the ratio of the DY Yield to the prediction from the templates. All uncertainties shown are statistical only.

	$0 < \mathrm{E_T^{miss}} < 30$	$30 < \mathrm{E_T^{miss}} < 60$	$60 < \mathrm{E_T^{miss}} < 80$	$80 < \mathrm{E_T^{miss}} < 100$
DY Yields	56620 ± 237.9	13843 ± 117.7	362 ± 19.0	34 ± 5.8
Templates	56769.0 ± 540.5	13725.9 ± 290.3	334.3 ± 31.7	25.7 ± 3.4
MC/BG	99.7 ± 1.04 %	100.9 ± 2.28 %	108.3 ± 10.83 %	132.5 ± 21.65 %
	$100 < \mathrm{E_T^{miss}} < 120$	$120 < \mathrm{E_T^{miss}} < 150$	$150 < \mathrm{E_T^{miss}} < 200$	$200 < \mathrm{E_T^{miss}}$
DY Yields	2 ± 1.4	0 ± 0.0	0 ± 0.0	0 ± 0.0
Templates	3.8 ± 0.58	1.9 ± 0.24	0.5 ± 0.09	0.1 ± 0.02
MC/BG	52.5 ± 72.34 %	0.0 ± nan %	0.0 ± nan %	0.0 ± nan %

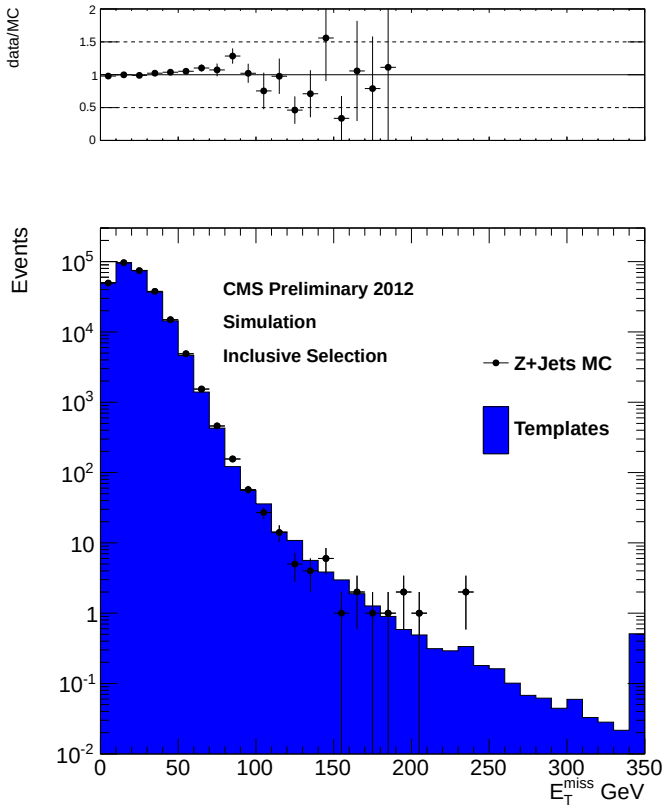

Figure 14: The E_T^{miss} distribution in Z + jets MC (black) and prediction (blue) using the inclusive analysis selection. See Table 18 for integrals.

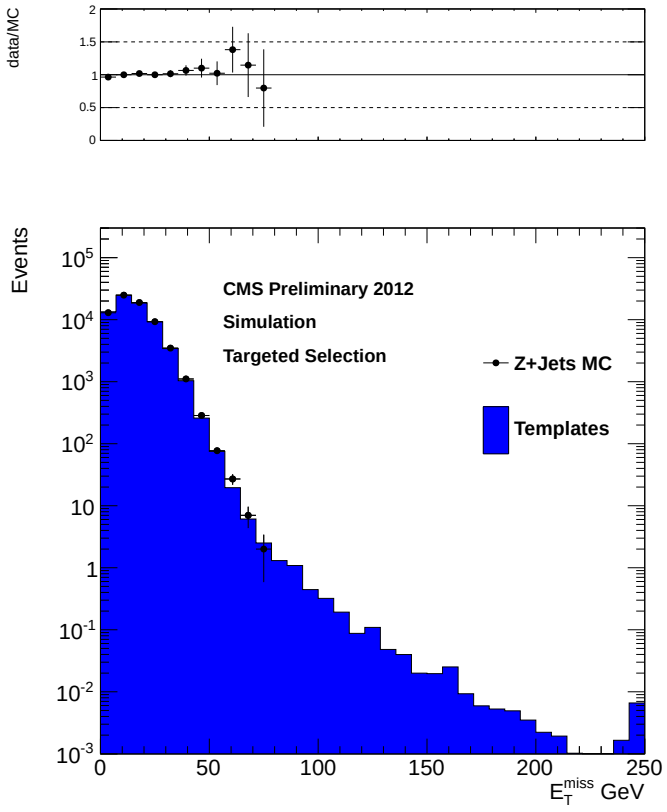

Figure 15: The E_T^{miss} distribution in Z + jets MC (black) and prediction (blue) using the targeted analysis selection. See Table 18 for integrals.

B Studies of Jets from Pileup

In order to ensure the jets which pass the jet selection are from the hard collision rather than from pileup (PU), we will require that the tracks in the jet are consistent with originating from the primary interaction vertex using the quantity β, defined below. In this section we study this quantity in MC.

The following dataset is used:

- `/DYJetsToLL_M-50_TuneZ2Star_8TeV-madgraph-tarball/Summer12_DR53X-PU_S10_START53_V7A-v1/AODSIM`

B.1 Selection

The preselection requirements from the inclusive analysis are used to study the PU jets, specifically:

- Require two leptons which both pass the lepton selection with $p_T > 20$ GeV/c
- 81 GeV $< M_{\ell\ell} <$ 101 GeV
- Require at least two jets both with $p_T > 30$ GeV/c and $|\eta| < 2.5$

B.2 Defining Jets to be "Matched" to Genjets

In order to determine which jets are from the hard collision and which jets come from PU using the MC truth information, the ΔR between each pfjet and the closest status 1 generator level jet with $p_T > 20$ GeV/c is calculated. By examining the distribution in Fig. 16 we choose a cut value of ΔR < 0.4 to define our jets as "matched" to a genjet, and if ΔR > 0.4, then the jet is defined to be a PU jet.

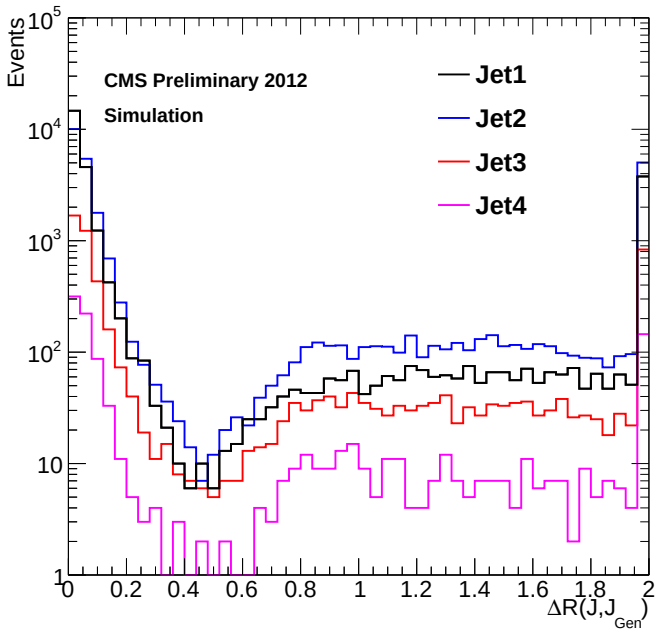

Figure 16: The ΔR for the four highest p_T jets is shown. We are using ΔR < 0.4 to define jets to be "matched" to a genjet.

B.3 Defining β

Now that we've established how to distinguish between PU jets versus hard scatter jets using MC truth information, we want to be able to be able to make the same distinction in data (without the truth information). In order to do this, the variable β is defined for each jet in equation (3)

$$\beta = \frac{\Sigma_i^{\mathrm{d_z}<0.5\ \mathrm{cm}}(p_T^i)^2}{\Sigma_i^{\mathrm{all}}(p_T^i)^2} \tag{3}$$

Jets with β close to 1 are jets from the hard collision, whereas Jets with β close to 0 are PU jets. By looking at the β distribution of the two highest p_T jets in Figure. 17, we choose a cut value of $\beta > 0.2$ to remove PU jets.

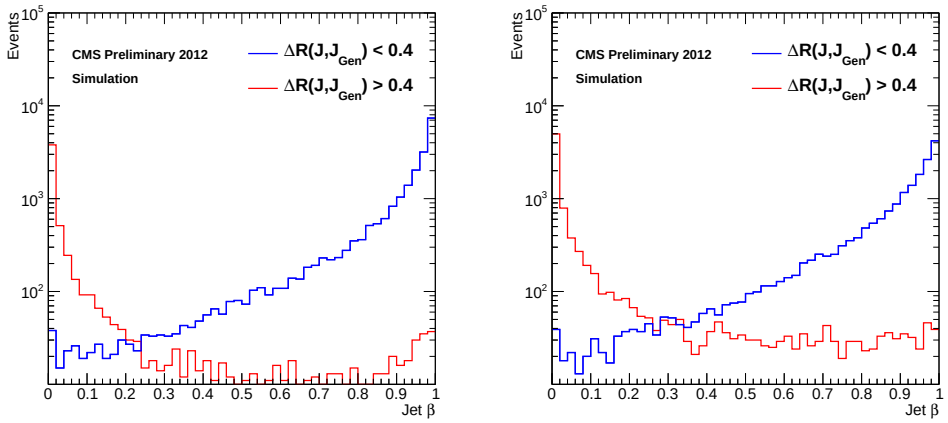

(a) (b)

Figure 17: β for jet1 (a) and jet2 (b).

We list the efficiencies for the β cut in table 20

Table 20: Selection efficiencies for a cut value of $\beta > 0.2$.

$\beta > 0.2$	PU Jets	Hard Scatter Jets
Jet 1	12%	99%
Jet 2	17%	99%

B.4 Dilepton p_T

These plots show the dilepton mass of events which pass the inclusive analysis selection. As you can see in Fig. 18, the PU jets have a significant contribution to the shape of the distribution at low p_T . The rejection of PU jets leads to a dilepton p_T distribution which looks healthy (i.e. the double peak structure is gone).

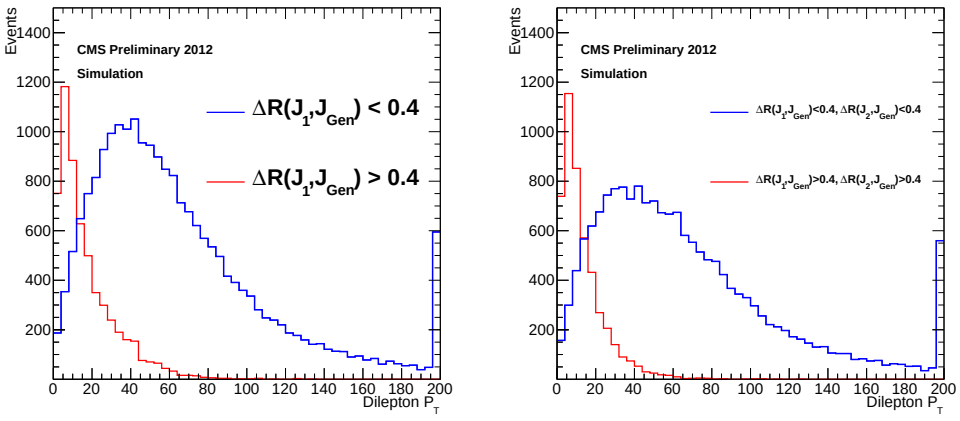

(a) (b)

Figure 18: Dilepton p_T with ΔR cut on jet1 (a) and ΔR cut on jet1 and jet2 (b).

B.5 Distinguishing Event Type

If we seperate the jets in the event by jet type (i.e. PU jets vs hard scatter jets), we can determine what type of event we are looking at. The possible event types are Z + 2 hard scatter jets, Z + 1 hard scatter jet and 1 PU jet, and Z + 2 PU jets. In Fig. 19, the ΔR between the highest p_T jet and its associated gen jet is plotted against the ΔR between the second highest p_T jet and its associated gen jet. We can use this plot to visually see the various regions which contain the three different event types.

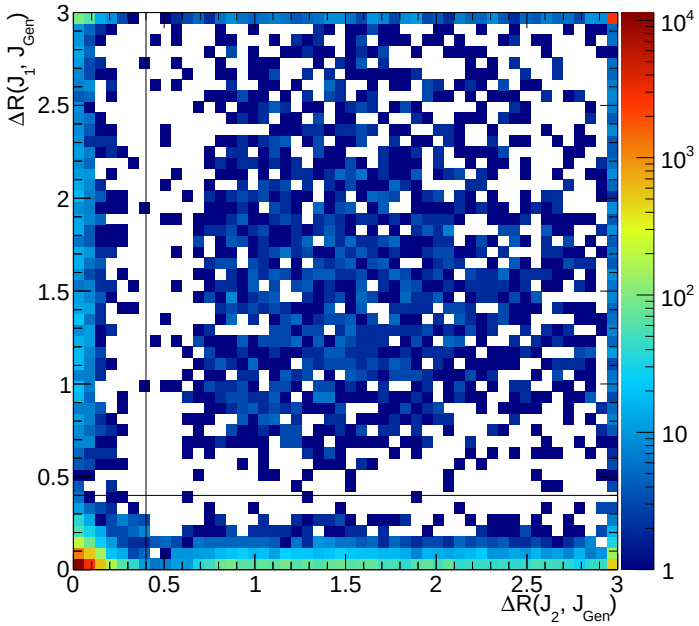

Figure 19: The ΔR(jet1, genjet) vs. ΔR(jet2, genjet)

We label the sections on this plot starting from the top left and going clockwise as sections 1 through 4. The events with 2 hard scatter jets are represented in section 4, the section with 1 hard scatter jet and 1 PU jet are represented in sections 1 and 3, adn the events with 2 PU jets are represented in section 2. Now we will look at $\Delta\phi$ between the 2 lead jets to see if we can better understand the events.

B.6 $\Delta\phi$ Between the Two Jets

In Fig. 20, we show the distribution of the $\Delta\phi$ between the two highest pt jets in the event.

These distributions represent the various sections in Fig. 19 as follows, section 1 is magenta, section 2 is red, section 3 is green, and section 4 is blue. The events in section 2 show a strong correlation for events to be back to back. The events in sections 1 and 3 show a flat distribution which implies that the jets ϕ is uncorrelated.

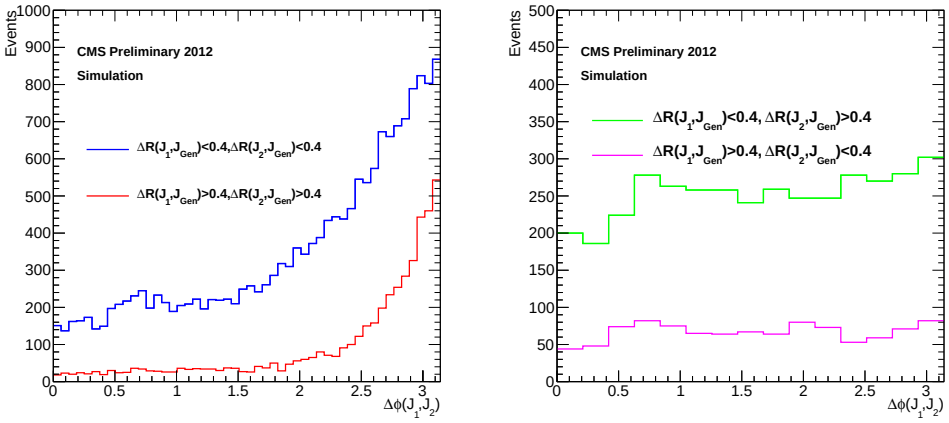

(a) (b)

Figure 20: The $\Delta\phi$ distribution between the two leading jets is shown in blue where both jets are matched to gen jets and shown in red for events where both jets are from PU in (a) and in (b) one jet is matched to a gen jet and the other jet is not matched to a gen jet.

C Results in the ee and $\mu\mu$ Channels

In this section we provide the results of the inclusive and targeted searches, separately in the ee and $\mu\mu$ channels. The $\mathrm{E_T^{miss}}$ distributions in the inclusive analysis for the ee channel are displayed in Fig. 21 and the signal region yields are presented in Table 21. The $\mathrm{E_T^{miss}}$ distributions in the inclusive analysis for the $\mu\mu$ channel are displayed in Fig. 22 and the signal region yields are presented in Table 22.

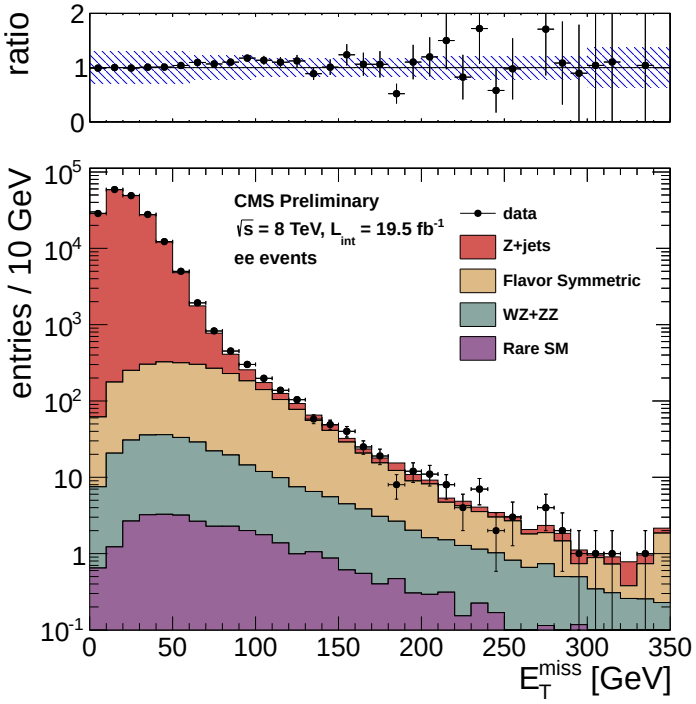

Figure 21: Results of the inclusive analysis in the ee channel. The observed $\mathrm{E_T^{miss}}$ distribution (black points) is compared with the sum of the predicted $\mathrm{E_T^{miss}}$ distributions from $\mathrm{Z}+\mathrm{jets}$, flavor-symmetric backgrounds, and WZ+ZZ backgrounds. The ratio of observed to predicted yields in each bin is indicated. The error bars indicate the statistical uncertainty in the data and the shaded band indicates the total background uncertainty.

Table 21: Summary of results in the inclusive analysis in the ee channel. The total background is the sum of the $\mathrm{Z}+\mathrm{jets}$ background predicted from the $\mathrm{E_T^{miss}}$ templates method ($\mathrm{Z}+\mathrm{jets}$ bkg), the flavor-symmetric background predicted from eμ events (FS bkg), and the WZ and ZZ backgrounds predicted from MC (WZ bkg and ZZ bkg). All uncertainties include both the statistical and systematic components. The Gaussian significance of the deviation between the data and total background is indicated for signal regions with at least 20 observed events.

	$\mathrm{E_T^{miss}}$ 0–30 GeV	$\mathrm{E_T^{miss}}$ 30–60 GeV	$\mathrm{E_T^{miss}}$ 60–100 GeV	$\mathrm{E_T^{miss}}$ 100–200 GeV	$\mathrm{E_T^{miss}}$ 200–300 GeV	$\mathrm{E_T^{miss}} > 300$ GeV
$\mathrm{Z}+\mathrm{jets}$ bkg	136452 ± 40942	43466 ± 13049	2220 ± 675	100 ± 57	5.1 ± 1.6	1.2 ± 0.4
FS bkg	431 ± 81	838 ± 156	896 ± 167	448 ± 84	22.5 ± 7.1	3.2 ± 1.9
WZ bkg	49.0 ± 24.5	83.6 ± 41.8	62.6 ± 31.3	35.7 ± 17.9	5.2 ± 2.6	1.5 ± 1.5
ZZ bkg	5.3 ± 2.7	11.9 ± 6.0	13.2 ± 6.6	13.3 ± 6.7	3.0 ± 1.5	0.9 ± 0.9
rare SM bkg	4.5 ± 2.3	9.7 ± 4.9	9.2 ± 4.6	8.4 ± 4.2	1.7 ± 0.8	0.5 ± 0.5
total bkg	136942 ± 40942	44409 ± 13050	3201 ± 696	606 ± 103	37.3 ± 7.9	7.3 ± 2.7
data	136404	44947	3508	651	42	3

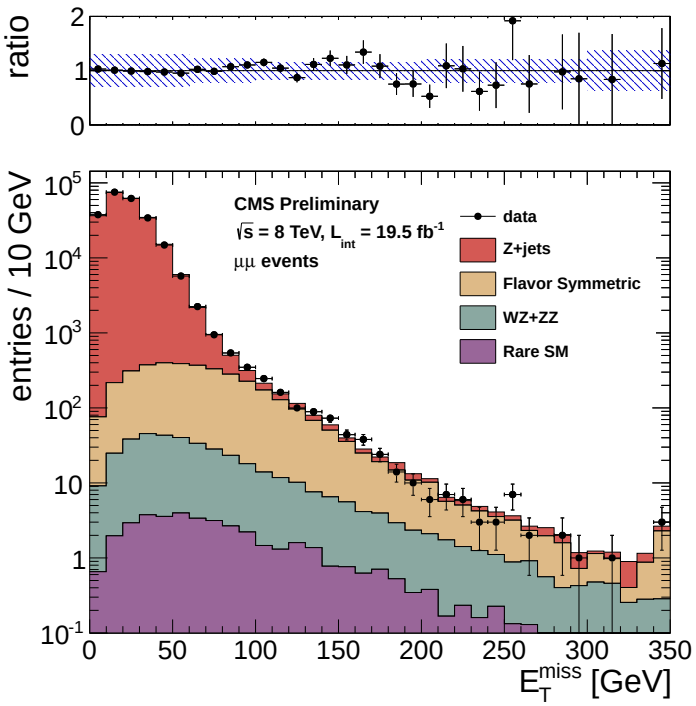

Figure 22: Results of the inclusive analysis in the $\mu\mu$ channel. The observed $\mathrm{E_T^{miss}}$ distribution (black points) is compared with the sum of the predicted $\mathrm{E_T^{miss}}$ distributions from $\mathrm{Z}+\mathrm{jets}$, flavor-symmetric backgrounds, and WZ+ZZ backgrounds. The ratio of observed to predicted yields in each bin is indicated. The error bars indicate the statistical uncertainty in the data and the shaded band indicates the total background uncertainty.

Table 22: Summary of results in the inclusive analysis in the $\mu\mu$ channel. The total background is the sum of the $\mathrm{Z}+\mathrm{jets}$ background predicted from the $\mathrm{E_T^{miss}}$ templates method ($\mathrm{Z}+\mathrm{jets}$ bkg), the flavor-symmetric background predicted from eμ events (FS bkg), and the WZ and ZZ backgrounds predicted from MC (WZ bkg and ZZ bkg). All uncertainties include both the statistical and systematic components. The Gaussian significance of the deviation between the data and total background is indicated for signal regions with at least 20 observed events.

	$\mathrm{E_T^{miss}}$ 0–30 GeV	$\mathrm{E_T^{miss}}$ 30–60 GeV	$\mathrm{E_T^{miss}}$ 60–100 GeV	$\mathrm{E_T^{miss}}$ 100–200 GeV	$\mathrm{E_T^{miss}}$ 200–300 GeV	$\mathrm{E_T^{miss}} > 300$ GeV
$\mathrm{Z}+\mathrm{jets}$ bkg	172758 ± 51829	54699 ± 16412	2752 ± 828	122 ± 44	6.2 ± 1.9	1.4 ± 0.5
FS bkg	531 ± 99	1032 ± 193	1105 ± 206	553 ± 103	27.7 ± 8.7	3.9 ± 2.4
WZ bkg	59.9 ± 30.0	102.8 ± 51.4	75.1 ± 37.6	43.0 ± 21.5	5.9 ± 3.0	1.6 ± 1.6
ZZ bkg	6.8 ± 3.4	14.7 ± 7.4	16.6 ± 8.3	16.5 ± 8.3	3.3 ± 1.6	1.1 ± 1.1
rare SM bkg	5.6 ± 2.8	11.3 ± 5.7	11.4 ± 5.7	9.5 ± 4.8	1.6 ± 0.8	0.6 ± 0.6
total bkg	173362 ± 51829	55860 ± 16413	3959 ± 854	744 ± 115	44.6 ± 9.6	8.7 ± 3.2
data	174626	54596	4070	799	37	4

The E_T^{miss} distributions in the targeted analysis for the ee channel are displayed in Fig. 23 and the signal region yields are presented in Table 23. The E_T^{miss} distributions in the inclusive analysis for the $\mu\mu$ channel are displayed in Fig. 24 and the signal region yields are presented in Table 24.

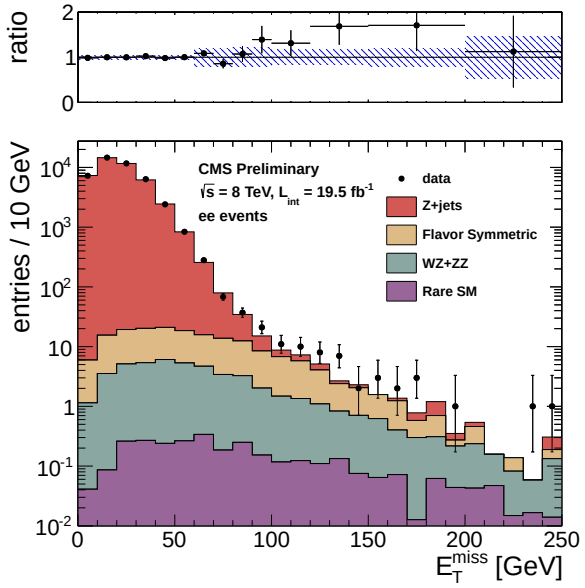

Figure 23: Results of the targeted analysis in the ee channel. The observed E_T^{miss} distribution (black points) is compared with the sum of the predicted E_T^{miss} distributions from Z + jets , flavor-symmetric backgrounds, and WZ+ZZ backgrounds. The ratio of observed to predicted yields in each bin is indicated. The error bars indicate the statistical uncertainty in the data and the shaded band indicates the total background uncertainty.

Table 23: Summary of results in the targeted analysis in the ee channel. The total background is the sum of the Z + jets background predicted from the E_T^{miss} templates method (Z + jets bkg), the flavor-symmetric background predicted from eμ events (FS bkg), and the WZ and ZZ backgrounds predicted from MC (WZ bkg and ZZ bkg). All uncertainties include both the statistical and systematic components. The Gaussian significance of the deviation between the data and total background is indicated for signal regions with at least 20 observed events.

	E_T^{miss} 0–30 GeV	E_T^{miss} 30–60 GeV	E_T^{miss} 60–80 GeV	E_T^{miss} 80–100 GeV
Z + jets bkg	33489 $\pm$ 1343	9401 $\pm$ 380	307 $\pm$ 68	28.8 $\pm$ 9.9
FS bkg	31.0 $\pm$ 6.2	42.9 $\pm$ 8.5	21.4 $\pm$ 4.3	15.6 $\pm$ 3.2
WZ bkg	8.0 $\pm$ 4.0	13.1 $\pm$ 6.6	6.0 $\pm$ 3.0	3.5 $\pm$ 1.7
ZZ bkg	1.4 $\pm$ 0.7	2.9 $\pm$ 1.5	1.5 $\pm$ 0.8	1.4 $\pm$ 0.7
Rare SM bkg	0.4 $\pm$ 0.2	0.8 $\pm$ 0.4	0.5 $\pm$ 0.3	0.4 $\pm$ 0.2
Total bkg	33530 $\pm$ 1343	9460 $\pm$ 380	336 $\pm$ 68	49.6 $\pm$ 10.5
Data	33420	9570	347	58
	E_T^{miss} 100–120 GeV	E_T^{miss} 120–150 GeV	E_T^{miss} 150–200 GeV	$E_T^{miss} > 200$ GeV
Z + jets bkg	3.5 $\pm$ 1.4	1.6 $\pm$ 0.7	0.9 $\pm$ 0.4	0.2 $\pm$ 0.2
FS bkg	9.7 $\pm$ 2.0	5.9 $\pm$ 1.3	2.5 $\pm$ 0.8	0.3 $\pm$ 0.2
WZ bkg	1.7 $\pm$ 0.9	1.5 $\pm$ 0.8	0.9 $\pm$ 0.4	0.4 $\pm$ 0.4
ZZ bkg	0.8 $\pm$ 0.4	0.8 $\pm$ 0.4	0.7 $\pm$ 0.4	0.7 $\pm$ 0.7
Rare SM bkg	0.2 $\pm$ 0.1	0.3 $\pm$ 0.2	0.3 $\pm$ 0.1	0.2 $\pm$ 0.2
Total bkg	16.0 $\pm$ 2.6	10.1 $\pm$ 1.7	5.3 $\pm$ 1.1	1.8 $\pm$ 0.8
Data	21	17	9	2

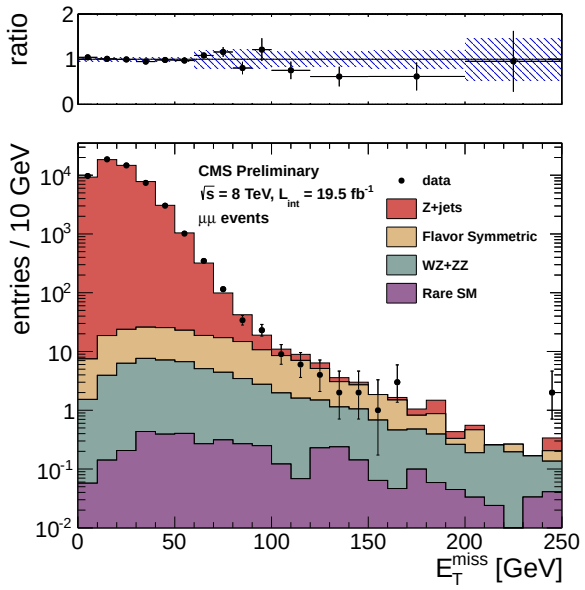

Figure 24: Results of the targeted analysis in the $\mu\mu$ channel. The observed $\mathrm{E_T^{miss}}$ distribution (black points) is compared with the sum of the predicted $\mathrm{E_T^{miss}}$ distributions from $\mathrm{Z}+\mathrm{jets}$, flavor-symmetric backgrounds, and WZ+ZZ backgrounds. The ratio of observed to predicted yields in each bin is indicated. The error bars indicate the statistical uncertainty in the data and the shaded band indicates the total background uncertainty.

Table 24: Summary of results in the targeted analysis in the $\mu\mu$ channel. The total background is the sum of the $\mathrm{Z}+\mathrm{jets}$ background predicted from the $\mathrm{E_T^{miss}}$ templates method ($\mathrm{Z}+\mathrm{jets}$ bkg), the flavor-symmetric background predicted from eμ events (FS bkg), and the WZ and ZZ backgrounds predicted from MC (WZ bkg and ZZ bkg). All uncertainties include both the statistical and systematic components. The Gaussian significance of the deviation between the data and total background is indicated for signal regions with at least 20 observed events.

	$\mathrm{E_T^{miss}}$ 0–30 GeV	$\mathrm{E_T^{miss}}$ 30–60 GeV	$\mathrm{E_T^{miss}}$ 60–80 GeV	$\mathrm{E_T^{miss}}$ 80–100 GeV
$\mathrm{Z}+\mathrm{jets}$ bkg	42346 ± 1699	11832 ± 479	383 ± 85	35.7 ± 12.3
FS bkg	38.2 ± 7.6	52.8 ± 10.5	26.4 ± 5.3	19.2 ± 3.9
WZ bkg	9.7 ± 4.8	16.7 ± 8.3	6.9 ± 3.5	3.9 ± 2.0
ZZ bkg	1.7 ± 0.8	3.5 ± 1.8	2.0 ± 1.0	1.8 ± 0.9
Rare SM bkg	0.4 ± 0.2	1.2 ± 0.6	0.6 ± 0.3	0.5 ± 0.3
Total bkg	42396 ± 1699	11907 ± 479	419 ± 86	61.2 ± 13.1
Data	42882	11421	462	57
	$\mathrm{E_T^{miss}}$ 100–120 GeV	$\mathrm{E_T^{miss}}$ 120–150 GeV	$\mathrm{E_T^{miss}}$ 150–200 GeV	$\mathrm{E_T^{miss}} > 200$ GeV
$\mathrm{Z}+\mathrm{jets}$ bkg	4.3 ± 1.7	2.1 ± 0.9	1.1 ± 0.5	0.2 ± 0.2
FS bkg	12.0 ± 2.5	7.2 ± 1.6	3.1 ± 0.9	0.4 ± 0.2
WZ bkg	2.3 ± 1.2	1.7 ± 0.9	1.1 ± 0.6	0.5 ± 0.5
ZZ bkg	1.1 ± 0.6	1.3 ± 0.7	0.8 ± 0.4	0.7 ± 0.7
Rare SM bkg	0.2 ± 0.1	0.6 ± 0.3	0.3 ± 0.2	0.2 ± 0.2
Total bkg	19.9 ± 3.3	13.0 ± 2.2	6.5 ± 1.3	2.1 ± 1.0
Data	15	8	4	2

D $\mathrm{E}_{\mathrm{T}}^{\mathrm{miss}}$ Templates from $\gamma + \mathrm{jets}$ Sample

In this section we display the templates used for the inclusive analysis (red) and the targeted analysis (blue).

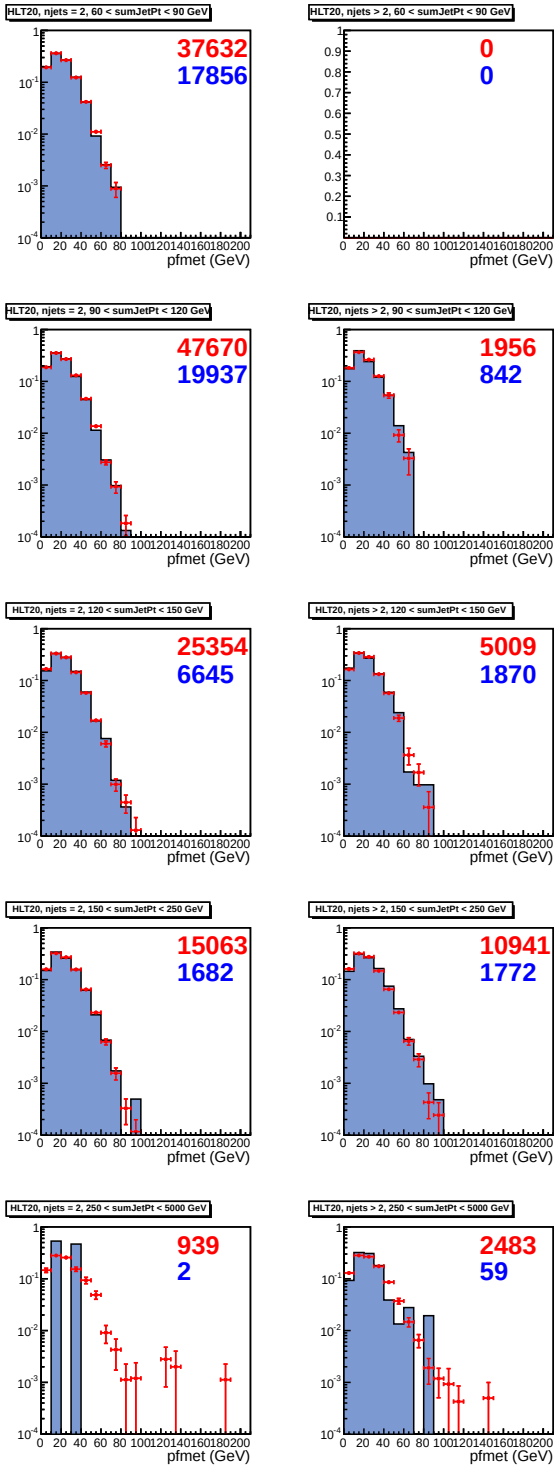

Figure 25: $\mathrm{E}_{\mathrm{T}}^{\mathrm{miss}}$ templates collected with the $p_T > 22$ GeV single photon trigger. The number in red (blue) indicates the number of entries in the template for the inclusive (targeted) analysis.

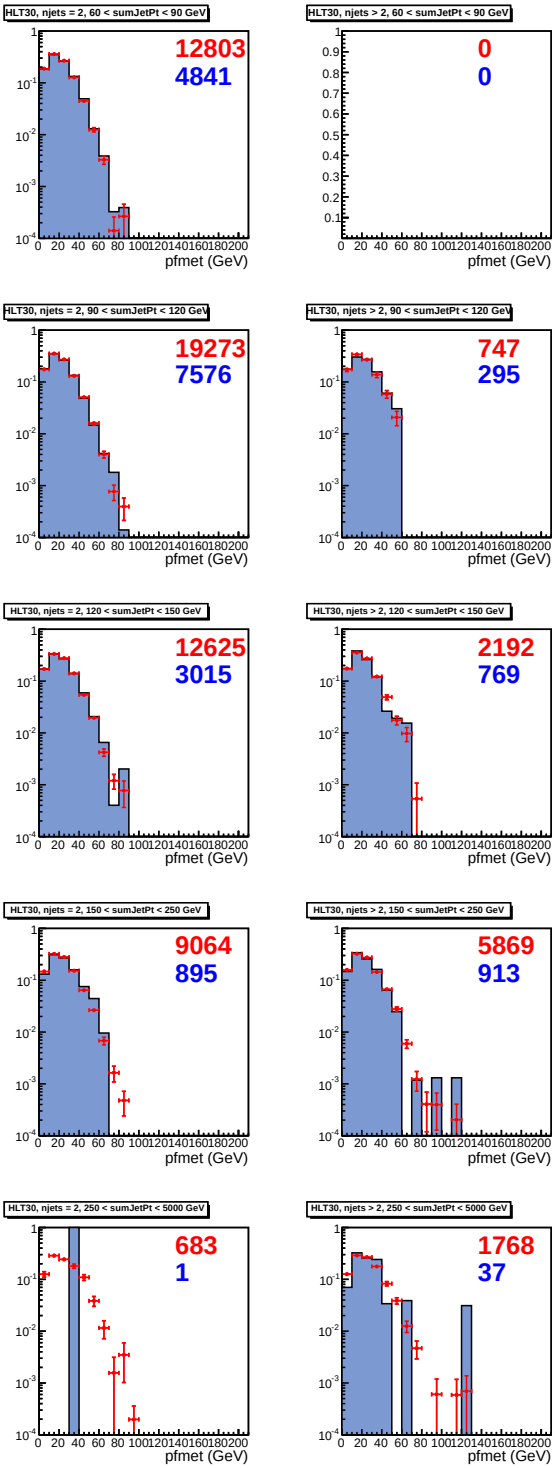

Figure 26: E_T^{miss} templates collected with the $p_T > 36$ GeV single photon trigger. The number in red (blue) indicates the number of entries in the template for the inclusive (targeted) analysis.

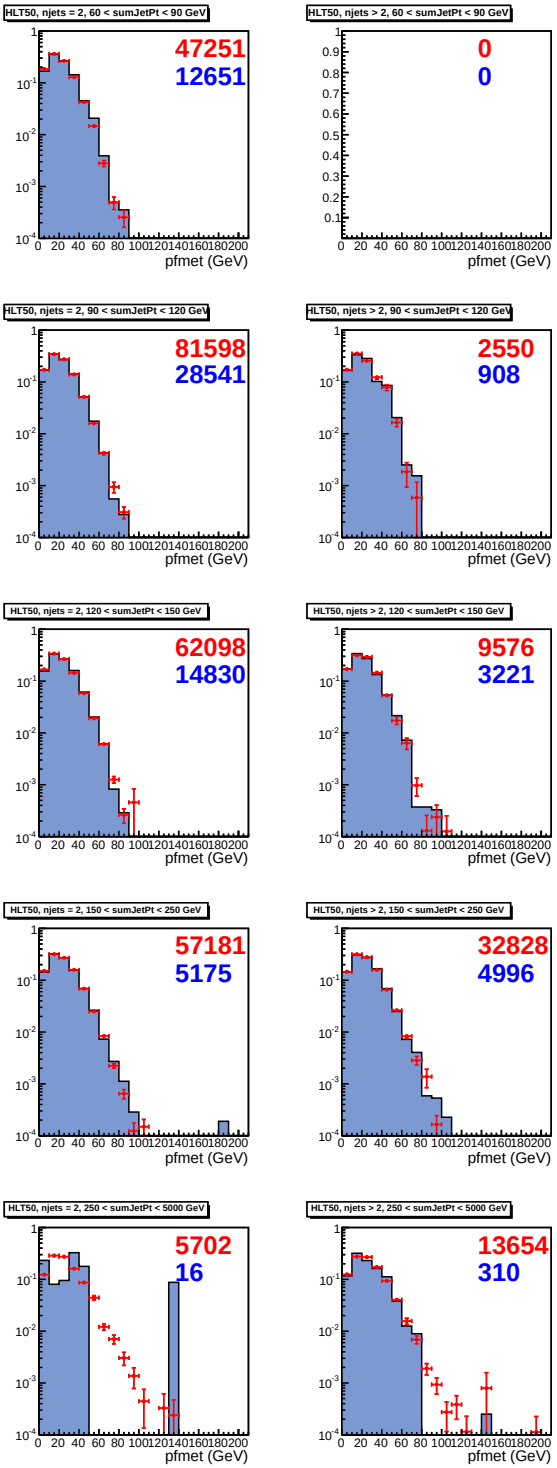

Figure 27: E_T^{miss} templates collected with the $p_T > 50$ GeV single photon trigger. The number in red (blue) indicates the number of entries in the template for the inclusive (targeted) analysis.

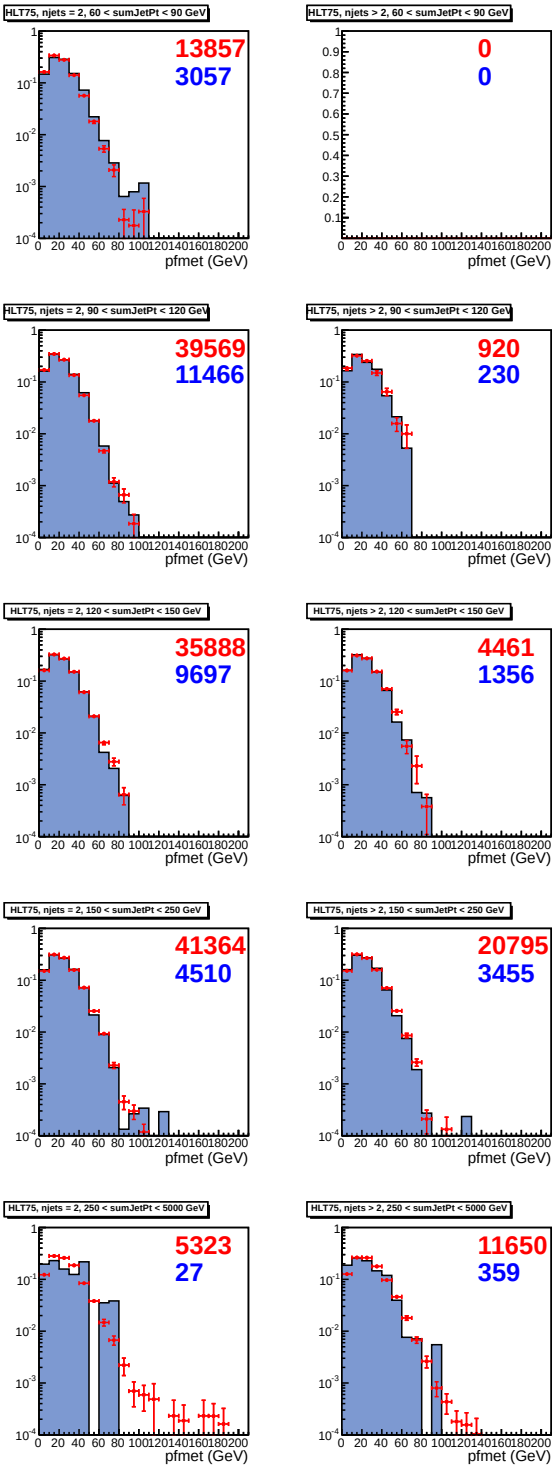

Figure 28: E_T^{miss} templates collected with the $p_T > 75$ GeV single photon trigger. The number in red (blue) indicates the number of entries in the template for the inclusive (targeted) analysis.

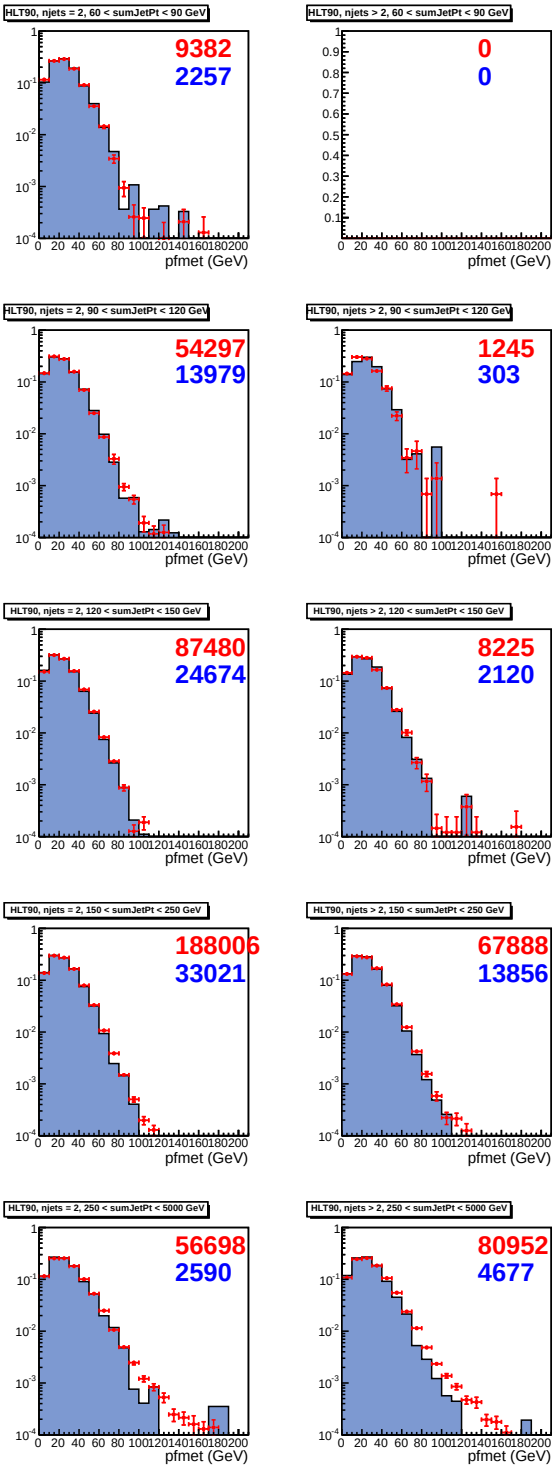

Figure 29: E_T^{miss} templates collected with the $p_T > 90$ GeV single photon trigger. The number in red (blue) indicates the number of entries in the template for the inclusive (targeted) analysis.